2006

Evaluating the deep-sea coral Acanella from Hawaii as a paleoceanographic archive

Geraldine Hourigan Lantier
University at Albany, State University of New York

Evaluating the Deep-Sea Coral Acanella From Hawaii as a Paleoceanographic Archive

Abstract of

a thesis presented to the Faculty

of the University at Albany, State University of New York

in partial fullfilment of the requirements for the degree of

Master of Science

College of Arts and Sciences

Department of Earth and Atmospheric Sciences

Geraldean Hourigan Lantier
2006

Evaluating the Deep-Sea Coral *Acanella* From Hawaii as a Paleoceanographic Archive

Geraldean Hourigan Lantier
2006

Abstract

Deep-sea corals have emerged as potential proxies of changing paleoceanographic properties. The utility of deep-sea corals for the purpose of interpreting paleoclimatic reconstructions is still in the discovery phase. However, long life spans, a relatively stable habitat, and unique growth geometry provide support to the growing body of research that has identified deep-sea corals as indicators of past climate and ocean properties. Two colonies of *Acanella* were collected from the permanent thermocline at depths between 414 and 437 m in the Makapuu Coral Bed, Oahu, HI in 1997 by submersible. Here I present results from a pilot study of the deep-sea coral *Acanella* to evaluate its use as a paleoceanographic archive. Commonly referred to as "bamboo coral" due to their alternating segments of calcite and gorgonin, *Acanella* was radiocarbon dated using samples from the protinaceous gorgonin knuckles. Scanning electron microscope (SEM) images, stable isotope data ($\delta^{18}O$ and $\delta^{13}C$), and a radiocarbon study of this azooxanthellate, ahermatypic coral were used to conclude that the vicinity where *Acanella* was growing in Makapuu Coral Bed most likely experienced significant shifts in thermocline depth over the course of the coral's lifespan. Samples were taken from the innermost and outermost growth bands of two *Acanella* thick sections (one from each colony studied here). These samples were corrected for a reservoir effect of 450 years and yielded an age of 270 +/- 35 years old for colony one and 22 +/- 35 for colony two. Colony one of *Acanella* may have recorded shifts in the thermocline near Hawaii as indicated by a 6˚ warming of ocean temperatures over 50 years. This warming trend was not observed in colony two, indicating that more information on growth geometry and deep-sea coral biology is needed in order to safely confirm that *Acanella* is consistently archiving paleoceanographic properties of the microhabitat in which the corals grow.

Evaluating the Deep-Sea Coral Acanella From Hawaii as a Paleoceanographic Archive

A thesis presented to the Faculty

of the University at Albany, State University of New York

in partial fullfilment of the requirements for the degree of

Master of Science

College of Arts and Sciences

Department of Earth and Atmospheric Sciences

Geraldean Hourigan Lantier
2006

Table of Contents

Page

List of Tables

List of Figures

Chapter 1
Introduction

Deep-sea corals can be found between 50 m and 4 km depth (Risk et al., 2002), as opposed to shallow-water, hermatypic reef-building corals that generally grow between zero and 20 m depth. Very little is known about the ecology, skeletal growth, and life span of deep-sea corals. Their remoteness makes monitoring deep corals *in situ* difficult. Druffel et al. (1995) refers to the deep-sea coral *Gerardia* as the Bristlecone pine of the deep sea. Similar to the Bristlecone Pine, some species of deep-sea coral such as *Acanella* are noted for their very slow growth rate and longevity, indicating that the skeleton of *Acanella* may be a potential paleoceanographic archive.

Many factors contribute to the geochemistry of a deep-sea coral's skeleton. It is known that water temperature, food availability, water depth, season, and absence of light, will influence deep-sea coral growth (Miller, 1995). Therefore, each coral skeleton can potentially archive a record of local oceanographic conditions specific to its habitat during its life. In *Acanella,* a record of both the surface and intermediate water properties can potentially be archived within the coral's skeleton because *Acanella* creates its skeleton from both sinking particulate carbon and dissolved inorganic carbon found in the water where the corals grow (Griffin and Druffel, 1989; Heikoop et al., 2002). The specimens of *Acanella* analyzed in this study were collected from depths between 414 m and 437 m in the Makapuu Coral Bed, Oahu, Hawaii. This depth range is within an interval in the water column of maximum vertical temperature gradient, known as the thermocline. *Acanella* is a stationary, solitary coral and continues to grow even as the

position of the main thermocline responds to overlying environmental and climate dynamics. Despite limited knowledge about *Acanella* skeletal accretion rates, growth geometry, general ecology, the location of *Acanella* in the water column, along with its slow growth, may make it a useful proxy for studying paleoceanography in the North Pacific. In this thesis the use of images generated from scanning electron microscopy (SEM), radiocarbon dating of individual thick sections of *Acanella,* and analysis of stable carbon and oxygen isotopes of the coral skeleton provide preliminary evidence in support of the use of *Acanella* as a recorder of paleoceanographic conditions.

Chapter 2
Oceanographic Setting

2.1 Makapuu Coral Bed

The Makapuu Coral Bed, 9 km off the northeast coast of Oahu, became a source for commercial harvesting of pink, gold, and bamboo coral starting in 1973 (Grigg, 1993). The Makapuu Coral Bed lies at 21°18.32' N, 157° 32.67' W (Figure 1).

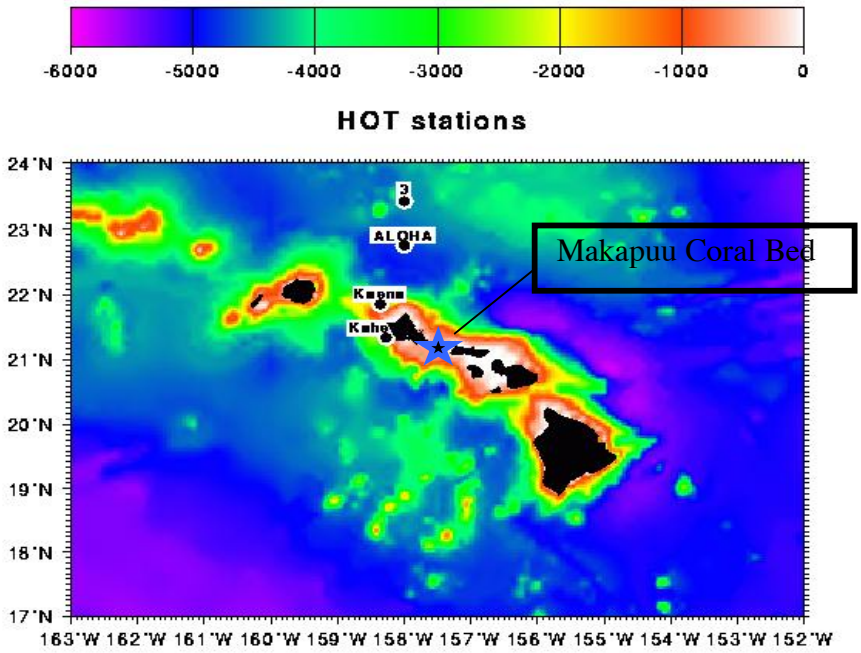

Figure 1. Bathymetry of the North Pacific surrounding the Hawaiian Islands (source: Hawaiian Ocean Time-Series http://hahana.soest.hawaii.edu/hot/hot.html).

The Makapuu coral bed is 3.6 km^2 in size and is located in the Makapuu Channel. The Channel is characterized by swift bottom currents of between 0-3 knots compared to 0-0.5 knots in 29 of 31 other corals beds in the Hawaiian Islands (Grigg, 1988). In

August 1997 a team of researchers aboard the submersible PISCES V dove as deep as 480 meters collecting various deep-sea coral species. Several colonies of *Acanella* were collected between 414 m and 437 m. Instrumental data gathered from Hawaiian Ocean Time-series Data Organization & Graphical Systems (HOT-DOGs) archive extend back to 1988 indicating that salinity in this depth range is between 34.07 and 34.13 p.s.u, and that ocean temperatures range between 7.3° and 9.4° C. If these corals can be used to reconstruct water temperature it may be possible to examine changes in thermocline depth over time.

2.2 Coral Collection Site and Vicinity

Hawaii is situated near the center of the North Pacific Subtropical Gyre located between ~ 15°N to 35°N longitude and 135°E to 135°W latitude (see Figure 2). The subtropical gyre covers $2x10^7 km^2$ and is one of the largest surface ocean circulation patterns on the planet (Karl and Lukas, 1996). The position of Hawaii with respect to this gyre is one reason for attempting to use deep-sea corals to reconstruct past changes in intermediate water in this region.

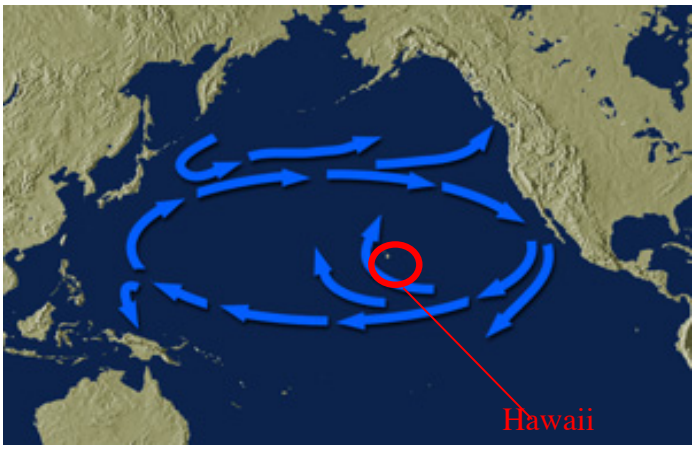

Figure 2. Illustration of ocean circulation in the North Pacific (source: http://www.aquatic.uoguelph.ca/oceans/PacificOceanWeb/NP%20Currents/Currenttypes.htm)

In 1988 a multidisciplinary deep-water oceanographic station, A Longterm Oligotrophic Habitat Assessment (ALOHA), was established at 22° 45'N and 158°00'W. The HOTs station ALOHA is located 100 km north of Oahu, and has instruments arrayed from the surface to 4800 m. Data recorded at the HOTs station ALOHA include conductivity, temperature, depth (CTD) profiling of temperature, salinity, and many other parameters including particulate abundances and related biogeochemical measurements. The goal of this program was to be able to design and maintain a deep-ocean hydrostation in the North Pacific in an effort to meet the objectives given by the U.S. Global Change Research Program (Karl and Lukas, 1996). Creators of the Hawaiian Ocean Time Series (HOTs) hoped to shed light on this area of the North Pacific that was once thought to be homogeneous and static. However, thanks to new instrumental data there now is new evidence that this mid-latitude gyre sustains substantial temporal and spatial physical and biological variability.

Karl and Lukas (1996) implemented ocean sampling stations in the North Pacific near Hawaii in order to constrain the time scale on which the thermocline changes position as well as to be able to understand more about what is forcing the changes in oceanographic properties at ~400 m. Changes in the North Pacific thermocline that occur on short time scales are believed to be the result of atmospheric and oceanic teleconnections from the tropics to the mid-latitude North Pacific Ocean (Miller et al., 1997). Teleconnections between the tropics and the North Pacific result from changes in surface wind stress or wind-stress curl (Trenberth, 1990). Such dynamics distribute heat over the Northern Hemisphere, thereby complicating interpretations for global warming and global climate change. It is possible that the interaction between ocean and

atmosphere causes changes in ocean circulation, ultimately changing thermocline depth over large areas of the North Pacific. One goal of this study of *Acanella* was to attempt to use geochemical variations in the skeleton of *Acanella* as a proxy for local and regional changes in thermocline conditions that might have implications for larger scale features of thermocline variability and climate change across the North Pacific.

The thermocline separates the warm upper ocean waters from the cold deep waters of the gyre. This gyre "tilts" poleward with increasing depth at higher latitudes. The Hawaiian Islands sit in an area that is south of the stagnation region that separates the North Equatorial current from the North Pacific current (Karl and Lukas, 1996). Hydrographic data collected at ALOHA for a study carried out by Kennan and Lukas (1996) showed that the station is recording data that is characteristic of the North Pacific Gyre. The two water masses observed at ALOHA are the North Pacific Tropical Water (NPTW) and the North Pacific Intermediate Water (NPIW). The NPTW is a high salinity surface water mass that forms as a result of excess evaporation near the subtropical front (Roden, 1979). The NPIW forms in the mixed water region between the Kuroshio and Oyahsio currents off of Japan. Near Hawaii, NPIW is found between depths 300 m and 700 m and is the main salinity minimum in the North Pacific (Kennan and Lukas, 1996). Research that followed the 1988 implementation of the HOTs program has proven that the area of the ocean surrounding the ALOHA station in the North Pacific traditionally thought of as a region with little variation in oceanic properties, was actually one of dynamic variability.

2.3 Thermocline

The thermocline is the layer or zone in the water column that has the steepest temperature gradient. The thermocline in the North Pacific ranges in depth from between 200 m and 1000 m depth, depending on overlying atmospheric conditions. In this study, *Acanella* was collected from the permanent thermocline, the part of the thermocline that sits below the more variable seasonal thermocline. The depth and temperature of the permanent thermocline in the region of the Makapuu Coral Bed varies due to ocean-atmosphere interactions in which winds create surface temperature gradients that in turn elevate or deepen the thermocline. There are many different ocean-atmosphere feedbacks that wind patterns can trigger, including thermocline shoaling, outcropping of the deeper, more permanent, thermocline waters at the surface, and low-level clouds that form over cold waters, all of which reinforcing cooler surface temperatures (note: this response is more likely south of the equator) (Federov and Philander, 2000). For this study site, average monthly temperature records were constructed from data archived in the Levitus "Major Ocean Parameters Files" Dataset found in the IRI/LDEO Climate Data Library (Figure 3). A slight shortening of the thermocline occurs during the January–March interval. It is possible that the shallowing seen in the January through March interval is the result of ENSO-related atmospheric circulation anomalies known to be the largest during December-February. Circulation anomalies are much weaker during the summer months (Alexander, 2003)

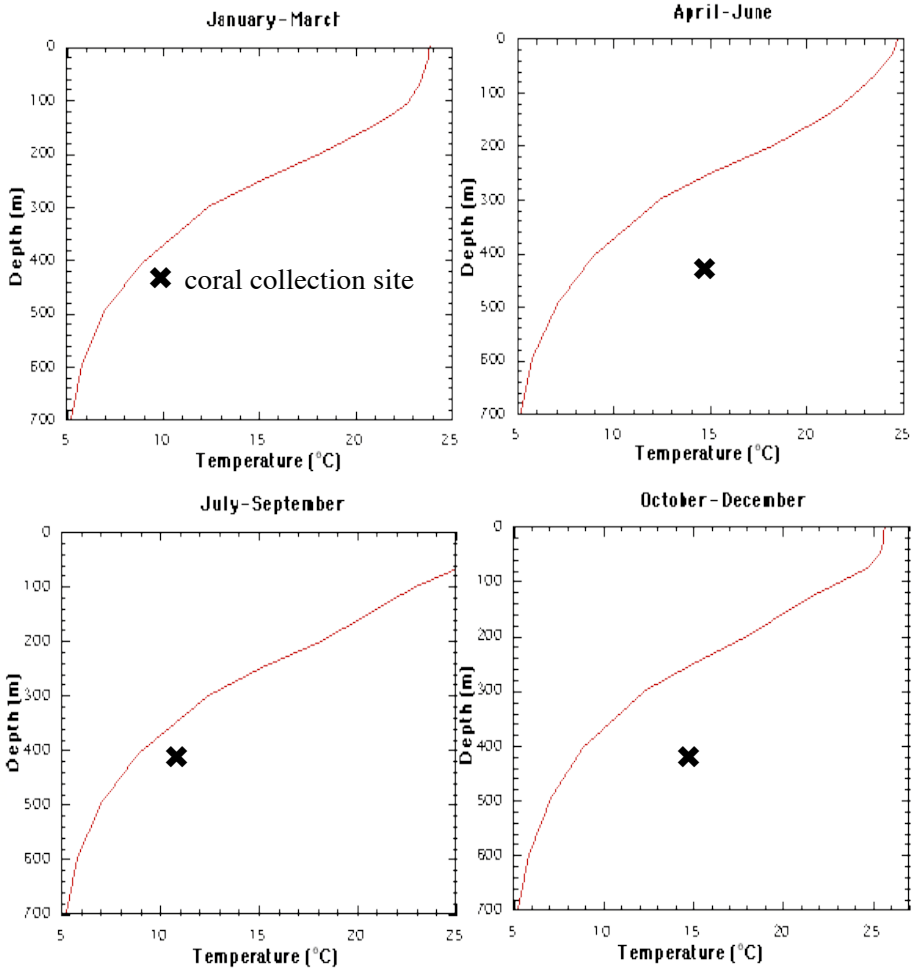

Figure 3. Seasonal thermocline climatology from 0-700 meters of water, 21°N, 157°W (Levitus et al., 1994, IRI/LDEO Climate Data Library)

On longer times than annual there are several studies that have linked thermocline depth to wind-stress curl whereby wind curl drives geostrophic currents by vertically displacing the thermocline. For example, Schneider and Miller (2001) found that during times of an anomalously deep Aleutian Low, the local intensification of the westerlies cool the interior North Pacific via enhanced surface heat flux to atmosphere. Eventually, Ekman pumping forces Rossby Waves to upwell, raising the thermocline and lowering

interior North Pacific sea surface temperatures (SSTs) (Mantua and Hare, 2002). These changes are likely associated with a ripple effect that emanates from the origination of El Nino events along the equator.

Variations in Western North Pacific thermocline depth have been described as interannual, basin-scale, east-west seesaw oscillations (Wang et al., 2000). This seesawing phenomenon and subsequent rising of the thermocline is also associated with wind-stress forcing. Surface wind variations also play a critical role in the movement of ENSO cycles.

2.4 Salinity

In this region of the North Pacific the surface ocean salinity maximum (~35 psu) lies under a long zonal band where there is a net loss of fresh water from the ocean to the atmosphere. The freshwater loss is attributed to northward Ekman flow driven by the easterly trade winds (Lukas, 2001). Lukas (2001) reported that wind, rainfall, and evaporation are all subject to interannual and decadal variability that can lead to low-frequency surface salinity changes at the ALOHA site. HOTs data shows a pronounced salinity decrease (~0.15 psu) in the upper pycnocline between 1991-1997, similar to the trend found in the central North Pacific Ocean that was suggested to be thermocline ventilation (Lukas, 2001) (Figure 4). If there was a freshening trend recorded at ALOHA at this time, it suggests that there was an anomalous subduction of relatively low salinity surface waters and due to change in Precipitation-Evaporation (P-E) balance. Lukas (2001) notes that in 1998 surface salinity increased and reached a maximum during a drought around the Hawaiian Islands. These salinity anomalies appear to propagate downward into the main thermocline with time (Figure 4). The delay in subduction of

salinity anomalies to reaching the ALOHA station ranges between one and four years (Lukas, 2001). In another study by Bingham and Lukas (1996), data taken from HOTs station ALOHA was used to describe annual variations of water mass properties in the North Pacific subtropical gyre. The NPIW has been defined by Sverdrup et al. (1942) as a salinity minimum in the depth range of 300-700 m, by Van Scoy et al. (1991) as the isopycnal σ26.8, and by Auad et al. (2003) as the salinity minimum between 33.9-34.4 psu salinity range. Figure 5 indicates that the *Acanella* specimens collected in this study between 415 and 430 m grew in water with a salinity of approximately 34.2 psu. (On average there is more pronounced salinity minimum from April to June.)

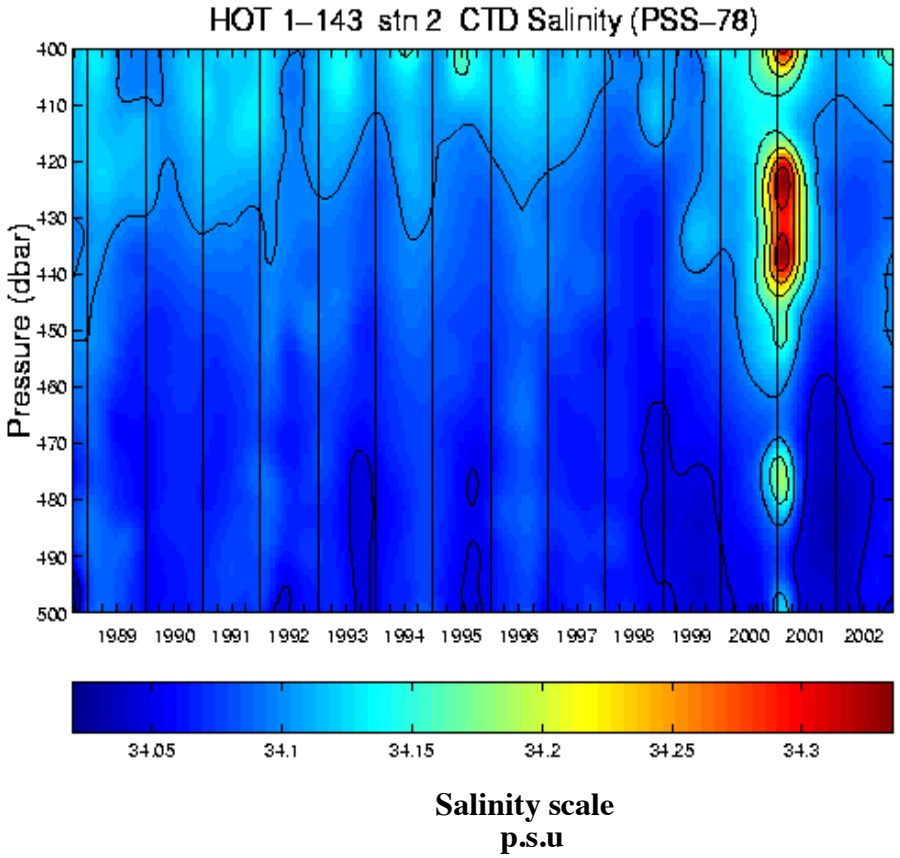

Figure 4. Data gathered from HOTs data archive using coordinates of the Makapuu Coral Bed show salinity between 400 and 500 m. Downward propagation of salinity changes are seen starting at 400 m. Downward propagation is most obvious during salinity maximum in 2001.

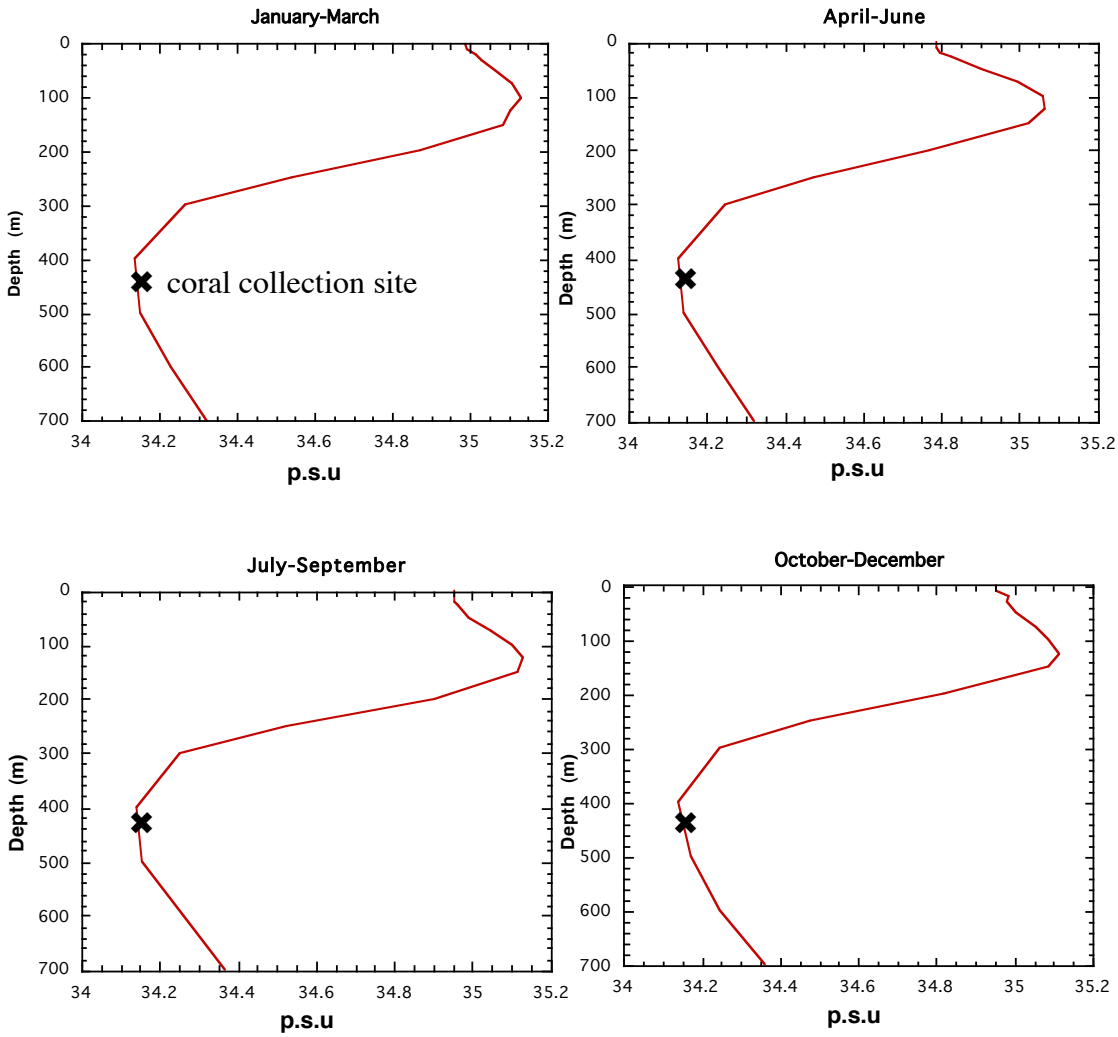

Figure 5. Monthly averages of salinity variability plotted using data archived in the Levitus Climatology (IRI/LDEO Climate Data Library). (Levitus et al., 1994)

Chapter 3
Acanella

Acanella is found within the subclass Ocotocorallia based on its unique formation of eight (octo) tentacles that stem from each polyp. All types of coral share similar polyp structures, such as an opening used both for feeding and excretion, simply referred to as the mouth, as well as tentacles that surround the body wall to help bring food in from surrounding water (Figure 6). *Acanella* is an ahermatypic or non-reef building coral. In order to develop their large fan-shaped structures, the corals need to situate themselves on a rocky substrate, with little or no sediment, below the photic zone.

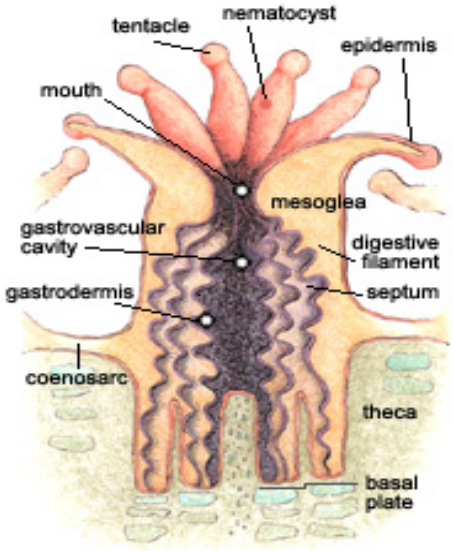

Figure 6. Basic structure of a coral polyp.
(ref:http://www.coris.noaa.gov/about/what_are/what_are.html)

Ahermatypic corals do not have algal symbionts, or zooanthellae, unlike reef-building corals. Since *Acanella* is an azooxanthellea species and does not require sunlight to reproduce or grow, it is able to live at depths between 400 and 1500 m (Grigg, 1993).

The branching arms of *Acanella* resemble sprawling candelabras (Figure 7). In solitary corals, one corallite is associated with each branching arm of the coral. Within each corallite, one polyp serves to protect the coral during coral growth.

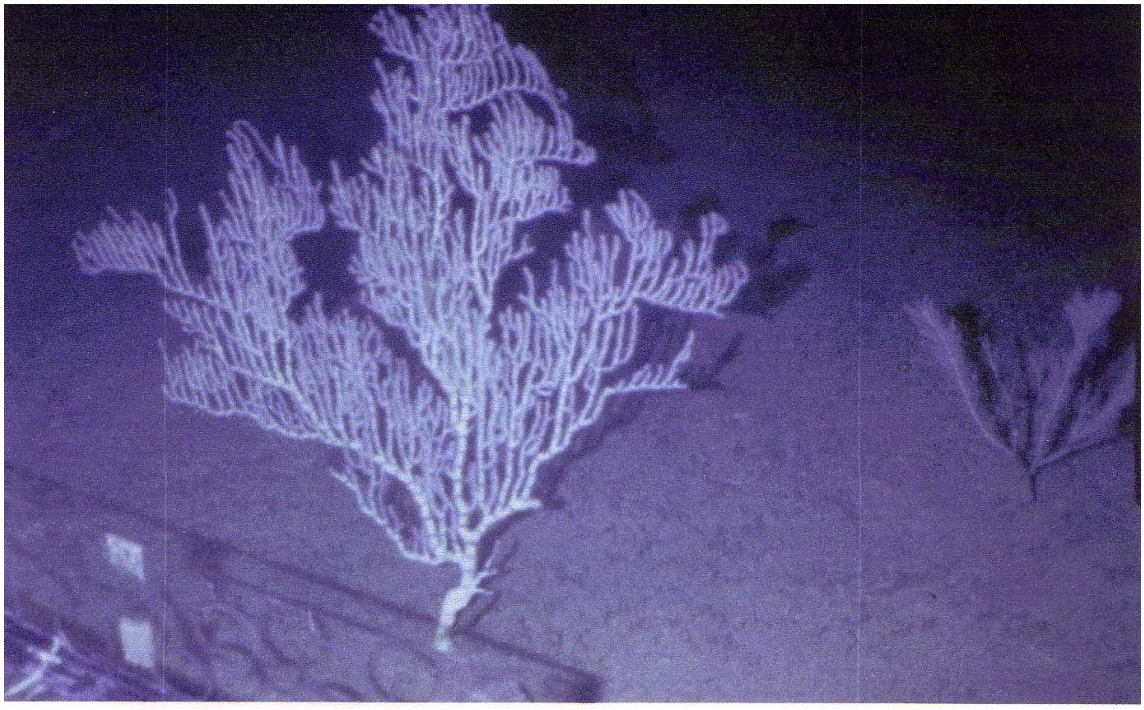

Figure 7. Photo taken of *Acanella* colony *in situ* before it was collected by external arm aboard the submersible vehicle PISCES V, August 1997, from the Makapuu Coral Bed, Hawaii. Photo taken by digital camera mounted on submersible.

Also unique to the subclass Octocorallia are their bony internodes, more commonly referred to as protein (gorgonin) knuckles (Figure 8). Due to the gorgonin knuckles, *Acanella* is more commonly known as bamboo coral because of its alternating segments of hard (white) calcite and proteinaceous (dark brown) gorgonin. Gorgonin is a "horn-like", fibrous protein that provides skeletal support for sea fans and other *Gorgonacea* corals. When the coral is living, the knuckles are flexible enough to allow

the corals to withstand currents without damage. Once collected, the coral's internodes dry, harden and separate from adjacent calcite nodes. The gorgonin acts as a mechanical support system allowing for enough flexibility within the coral skeleton in order to position its polyps for feeding in various water velocities in this region (Lewis et al., 1992). It is not known exactly what causes *Acanella* to alternate between calcite and gorgonin when accreting its skeleton. Risk et al. (2002) suggested that alternating segments could be based on temporal variations in the influx of sediments into the channel where the Makapuu Coral Bed is located. Spero et al. (2003) indicated that calcite and organic internodes of the skeleton are precipitated simultaneously based on his findings that the calcite and protienaceous internodes have chemistries that are temporally coupled. Lewis et al. (1992) noted that the accretion of calcite and gorgonin in deep-sea corals in the subclass Octocorilla occurs in concentric layers around a central, hollow, chambered canal that seldom exceeds 100 μm in diameter (Figure 9). The *Acanella* colonies studied here all posses the perfectly circular chamber described above as well as growth bands found in various widths in both the calcite and gorgonin parts of the coral skeleton.

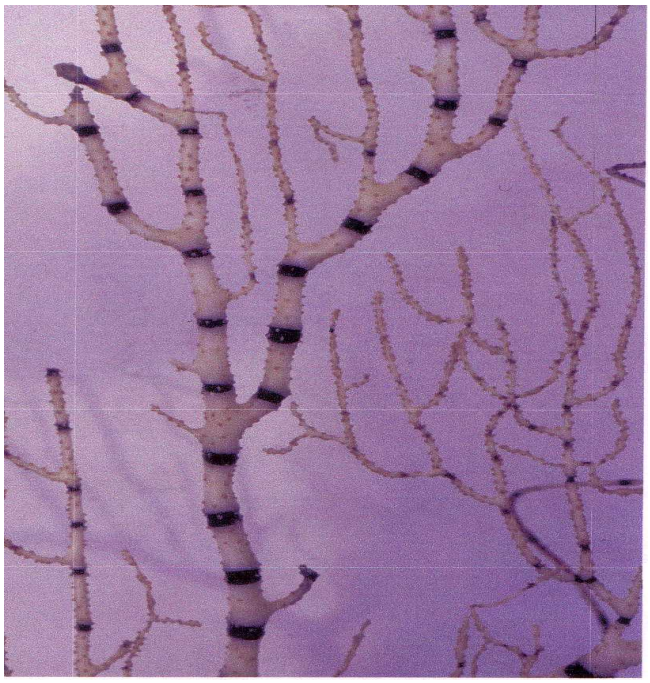

Figure 8. Close up photograph of *Acanella*. Further illustrates branching and alternating nodes of calcite and gorgonin in coral colony.

Developing a better understanding of *Acanella* skeletal structure is imperative for distinguishing growth banding during micromilling of the calcite nodes. It is known that deep-sea corals form the basis of their skeleton with the basic trabecular unit. The trabeculea are composed of small bundles of fibrous rods that compose the framework of the coral's skeleton. However, the exact ordering and arrangement of the rest of the skeletal growth features remains to be determined and currently limits the utility of *Acanella* for time series reconstructions of ocean properties.

3.1 Growth Banding

Acanella accretes concentric calcite and gorgonin rings extracellularly (Lewis et al., 1992). The rings are separated from the cell cytosol by a membrane. The enzyme ATPase (of the nucleotide adrenosine triphosphate) is responsible for the active transport of Ca^{2+} through the membrane that acts as a barrier between the basal ectoderm and the

skeleton in an area called the sub-membrane space that is in direct contact with seawater (McConnaughey 1988, 1989b). Within the calcite nodes, growth bands are accreted in successive concentric rings. Each band that is successively accreted seals the previously deposited growth feature, not allowing for any dissolution or contact with the tissue layer where new skeleton is being formed (Lazier et al., 1999). Very fine calcite septa radiate from the center of the coral (Figure 9).

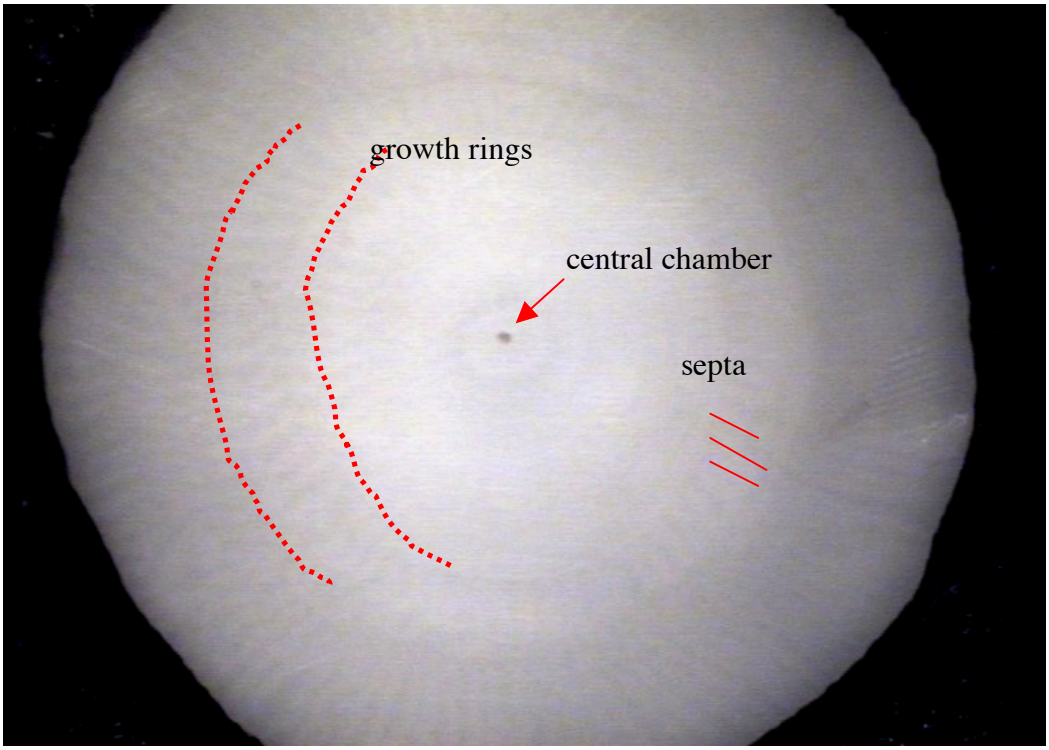

Figure 9. Digital image of *Acanella* in thick section. Image shows concentric growth bands as well as fine septa radiating from the center of the specimen. Photo was taken by digital camera that is part of the micromilling apparatus, prior to milling of this particular specimen.

The gorgonin knuckles found in *Acanella* contain fine-scale growth structures (see Figure 8). While the periodicity of these growth patterns in both the calcite and gongonin skeletal segments is unknown, the presence of well-defined growth structures suggest the growth rings may be related to changes in external environmental conditions

and that *Acanella* may have deposited its skeleton in a continuous and sequential manner. This situation potentially allows for the utilization of the skeleton for high-resolution time series reconstructions of temperature and ocean chemistry.

The thickness and density of growth bands in ahermatypic corals is related to nutrient availability, food supply, and to environmental stressors. Stress events could be related to cold-water incursions or other events related to large-scale climate changes. A study by Lazier et al. (1999) attempted to discern the skeletal architecture of the solitary deep-sea coral *Demopyllum cristagalli*. This study showed that *D. cristagalli,* grows by secreting growth bands in layers between the tissue layer and the skeleton. These researchers were not able to find any conclusive evidence for annual growth banding or reasons for differing thicknesses or frequency of well-defined growth bands.

Growth rate measurements for deep-sea corals are orders of magnitude lower than those for hermatypic corals growing in the surface ocean reef environment. For example, the deep-sea coral *Corallium niobe* has been determined to have a trunk growth rate of 0.11 +/- .02 mm/yr over a 200 year period based on excess ^{210}Pb measured in concentric bands (Druffel et al, 1990). This compares to surface dwelling coral's skeletal growth of 2-25 mm based on annual growth bands (Grigg, 1994).

Grigg (1994) was able to estimate that the most mature corals found in the Makapuu Coral Bed were at least 75 years old. Grigg (1974) employed several different methods to determine the relative ages of Hawaiian deep-sea corals found. These include identifying corals living on hard substrates of known age, comparing of growth ring counts between specimens of the coral, measuring annual skeletal regeneration on cut surfaces, and using simple height measurements averaged annually. Results of this series

of studies showed that two colonies situated as close together as 3 m could vary tremendously in growth rate. One cause of this might be differences in food supply or other aspects of changing microhabitat. Grigg (1974) noted that due to the remoteness of deep-sea coral colonies, differences in growth banding may be related to biological changes versus physical oceanographic changes at ~400 m.

Chapter 4

Context of Climate Variability: North Pacific

Lukas and Santiago-Mandujano (2001) observed high salinity, high temperature, low oxygen, and elevated fluorescence between 300 and 550 m water depth just north of the Makapuu Coral Bed at Station ALOHA (22°54'N, 158°W). These conditions were recorded during January 2001. Researchers hypothesized that the salty, oxygen-depleted waters were transported from south of Baja California northward in the California Undercurrent during the strong El Nino event in 1997-1998. Although this particular event does not affect the corals studied here, incursions of anomalous water masses may have been present during the lifespan of the *Acanella* analyzed in this study.

HOTs and ALOHA data do not indicate the presence of temperature or salinity anomalies in the thermocline associated with recent ENSO events. In this region teleconnections are important in terms of SST and precipitation anomalies in the North Pacific (Trenberth, 1990). The Pacific North American (PNA) teleconnection pattern is one of the most prominent modes of low-frequency variability in the Northern Hemisphere extratropics, and is most prominent from March to July. Lower frequency "ENSO-like" events can persist for 20 and 30 years versus the commonly observed duration of an El Nino event of 2-7 years (Mantua and Hare, 2002). These "ENSO-like" phases are caused by the alternation between positive and negative regime shifts and intensification of the Pacific jet stream, followed by the enhanced cyclonic circulation over the southeastern United States. This alternation between warm (positive) and cold (negative) phases in the North Pacific surface ocean is referred to as the Pacific Decadal Oscillation (PDO) (Mantua et al., 1997).

The PDO is a term that was first used by fisheries scientist Steven Hare in 1996. The PDO is referred to as a long-lived El Nino-like pattern of Pacific climate variability. PDO and ENSO climate patterns may persist for 20-30 years and 2-7 years respectively. Additionally, climatic fingerprints associated with either the warm or cold phase of the PDO are most prevalent in the North Pacific, with secondary manifestations in the tropics, the opposite of the case for ENSO. The presence of PDO and secondary ENSO signals in the Eastern North Pacific indicates that climatic changes in this region occurred over several different time scales where *Acanella* grew. Further, the Hawaiian Islands are located near the correlation hinge point for PDO and Interdecadal Pacific Oscillation (IPO) patterns in SST making it difficult to correlate SST patterns near Hawaii with those in the North or South Pacific. IPO has a similar pattern to that of the PDO, but has a cycle of 15-30 years and affects both the North and South Pacific. Researchers including Nitta and Yamada (1989), Trenberth (1990), and Miller et al. (1997) described a major "climate regime shift" during 1976/1977 (Figure 10). Although this shift was first noted along the equator, the PDO also reversed phase in 1976, affecting much of the surface ocean in the Pacific basin. When Mantua et al. (1997) first began studying PDO it was thought that climatic fingerprints were most pronounced in the North Pacific/North America, with only loosely connected manifestations in the Southern Hemisphere. Examination of North Pacific SST data shows that there is the potential for two different centers of PDO action, one of which encompasses the region near the ALOHA station, the subtropical front of North Hawaii, the other is located near the subarctic front that defines the Kuroshiro/Oyashio Extension (Mantua and Hare, 2002).

The IPO was first named in 1999 and is thought to be the Pacific-wide manifestation of the better known Pacific Decadal Oscillation (PDO), implying that PDO may be an

incomplete description of a much wider climatic phenomenon. Both phenomena changed phase near the time of the Pacific "climatic shift" around 1976. Although it remains unclear to what extent either phenomenon is physically separate from ENSO fluctuations, the IPO was shown a few years ago to modulate high- frequency ENSO rainfall teleconnections to Australia in an apparently rather strong way. Such results have recently resulted in the use of the IPO concept in paleoclimate studies (Folland et al., 2002).

Recent studies of proxy data for marine ecosystems in the North Pacific have included recruitment and population studies of salmon stocks of the west coast of North America. Major findings showed that the warm phase of the PDO favors high production of Alaskan salmon stocks, whereas cold phases have the opposite effect on salmon population in Washington, Oregon, and California (Mantua et al., 1997; Hare et al., 1999). While there have been no fish stock studies near the Hawaiian Islands, historical records tracking aspects of Pacific marine ecosystems suggest a strong association between PDO variability and seabird population, (Vanderbosch, 2000). In Honolulu, Hawaii researchers noted that Christmas Bird population dropped off following a strong ENSO in 1982-1983. Researchers go on to link longer-term variability with phases of the PDO noting that the bird populations are suppressed during the warm phases.

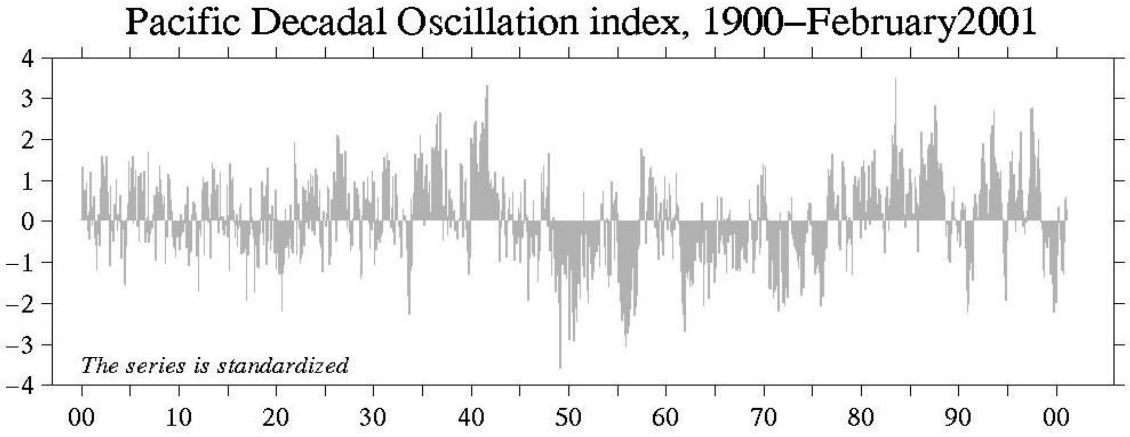

Figure 10. PDO Index showing pronounced regime shift in 1976-1977. (Mantua et al. 1997)

Chapter 5

Deep Sea Corals as a Paleoarchive

Deep corals are potentially good archives for reconstructing the circulation of the deep sea because they are undisturbed by bioturbation (Mangini et al., 1998). Some records obtained from surface-dwelling corals have to be pieced together due to fish grazing that disturbs the continuous growth of a coral. Deep-sea ahermatypic corals are not restricted to certain depths, and can be found in temperatures ranging from -1° to 28°C (Stanley and Cairns 1988), making it possible to establish comparisons between several different species of deep-sea corals for a more comprehensive look at their utility as indicators of climate change.

Risk et al. (2002) examined growth rates of two deep-sea gorgonin corals, using scanning electron microscopy (SEM) to image annual growth rings within the structure of the coral skeleton. Within the large annual bands, fine couplets of gorgonin are observed. The results from this study allowed for a more detailed analysis of the skeletal structure and growth ring morphology of deep -sea corals. The corals studied, *Primnoa resedaetermis* and *Desmophyllum cristagalli* had skeletal compositions that resembled the protein nodes within the *Acanella* skeleton.

Druffel (1986, 1990, 1995, 2001) and Griffin and Druffel (1989) used tracers such as radiocarbon to investigate sources of carbon in the deep sea. Major findings from these studies revealed that deep corals, especially those that contain both calcite and proteinaceous knuckles reminiscent of those seen in *Acanella,* are actually utilizing more than one reservoir for incorporation of carbon during skeleton building or nutrient ingestion. The aforementioned studies also used analysis of radiocarbon and $\delta^{13}C$ isotopes from deep-sea corals as markers of inputs of CO_2 from the atmosphere. Measurements

taken from a Hawaiian surface coral showed a 7‰ decrease in $\Delta^{14}C$ during the time between AD 1893 and 1952. This decrease is consistent with the Suess Effect, or the dilution of natural levels of ^{14}C by ^{14}C-free fossil fuel generated CO_2. These findings go on to infer that the subtropical gyre and vertical mixing in the North Pacific is the likely physical mechanism for variation seen in the radiocarbon signatures in these corals.

In another study of deep-sea corals collected from the Makapuu Coral Bed, Roark (2003) radiocarbon dated and measured oxygen ($\delta^{18}O$) and carbon ($\delta^{13}C$) stable isotopes of *Corallium* and *Gerardia*. *Corallium* is a calcitic coral that was found to be much younger than the *Gerardia*, also collected from the middle of the permanent thermocline, with a value of 835 ^{14}C years along a radial transect at the base of the coral stalk. *Gerardia*, a protinaceous zooanthid coral, measured 1200 ^{14}C years along a 12mm transect across the base of the coral stalk. The presence of bomb carbon in the outer edge of the coral suggests that surface derived particulate organic carbon (POC) is the primary source of carbon to the *Gerardia* skeleton. In contrast, the presence of bomb ^{14}C equivalent to that of post-bomb radiocarbon values at 400m suggests that *Corallium* utilizes carbon from surrounding water that was initially transported from the surface. Although Roark (2003) did not analyze *Acanella,* by inference their results suggest that the carbon in the calcite portion of *Acanella* may be derived from the dissolved inorganic carbon (DIC) pool surrounding the coral at ~400m. The protineaceous (knuckle) portion of *Acanella* derives its particulate organic carbon (POC) from the surface. Additionally, oxygen isotope data in Roark (2003) indicate that the range in $\delta^{18}O$ values could be explained by a 4° temperature change which they attribute to changes in the thermocline depth in this area.

Adkins et al. (1998) collected deep-sea corals from the western North Atlantic in order to characterize the role of the deep ocean during abrupt climate changes such as the Younger Dryas (~ 13,000—11,700 calendar years B.P.). Using coupled radiocarbon and ^{230}Th dating, they were able to narrowly constrain the timing of the ventilation of the North Atlantic upper deep water in a narrow window of time. From these ages, and Cd/Ca data, they were able to show that the deep ocean was ventilating on decadal-centennial time scales while rapid changes were occurring at the sea surface and in the atmosphere.

Adkins et al. (2002) described in more detail the use of North Atlantic deep-sea corals as paleoceanographic archives. Deep-sea corals in this study were used as a tracer of Δ^{14}C and bomb-produced ^{14}C in the ocean. Their work addressed the question of whether deep-sea corals are recording the radiocarbon value of ambient DIC as the coral builds its skeleton. Adkins et al. (2003) used deep-sea corals to examine biological vital effects during the formation of their skeleton. The study points out that vital effects are apparent in some, but not all, species of deep-sea coral.

Deep-sea corals grow at depths in the ocean that undergo little change in water temperature, salinity, and seawater oxygen isotopic composition, potentially simplifying analysis of the vital effects in *Acanella* for example. That said, deep-sea corals can live for decades and even for several centuries. Should there be a large change in surrounding water temperature, isotopic composition of the water, or an influx of bomb carbon, these changes could be recorded in the skeleton of the coral.

Chapter 6
Methods

6.1 Collecting Acanella

Acanella specimens were collected on August 21, 1997 during a Hawaii Undersea Research Laboratory/NOAA funded submersible dive aboard the vessel PISCES V. Several different species of deep-sea coral were collected using an external arm. All coral species were living when they were harvested.

6.2 Instrumental Data

General Oceanics 24-place pylon and an aluminum rosette containing 24 PVC bottles were used to obtain water samples at various depths. The rosette was deployed on a 3-conductor cable allowing for real-time data to be observed. Once deployed, operators can trip the bottle tops at different depths in order to sample various locations in the water column (Karl and Lukas, 1996). Samples were collected from the surface to within 50m of the seafloor.

6.3 Preparing/Micromilling Acanella Sections

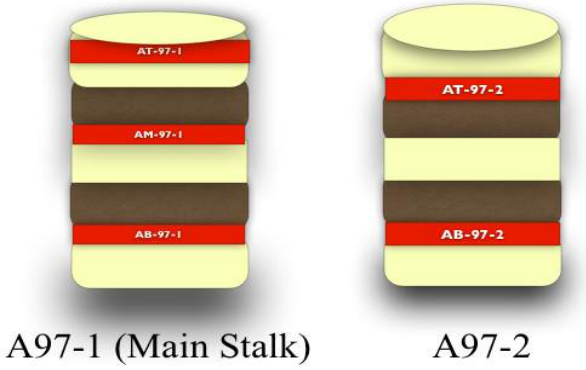

Figure 12. Coral sampling map (not drawn to scale). Sub-samples for the purpose of radiocarbon dating were taken from AM97-1 and AT97-2. Red indicates portions of the skeleton sampled for stable isotope analysis, brown indicates protein "knuckles", white indicates calcareous skeleton.

Two colonies of *Acanella* designated A97-1 and A97-2 were analyzed as part of this study. The basal stalk of A97-1 was sectioned at the top, middle, and bottom into ~3mm thick sections, while A97-2 was similarly sectioned at the top and bottom of its basal stock (see Figure 12).

The portion of the stalks that were sub-sectioned for analysis of $\delta^{13}C$ and $\delta^{18}O$ and Scanning Electron Microscope (SEM)/Energy Dispersive Spectroscopy (EDS) were ~ 2-3cm in diameter. Sections were polished with successively with aluminum polishing grit of decreasing size from 320-1000 mesh, to eliminate saw marks and enhance growth banding. Sections were then mounted on microscope slides using epoxy.

6.3.1 Sample Preparation for Isotope Analysis

Micromilling of samples was carried out at the Lamont Doherty Earth Observatory, Columbia University using a Merchantek Micromill Sampling System in the laboratory of Dr. Peter deMenocal. Samples mounted on a robotic stage were viewed and digitized in real-time using a high-resolution Y/C color CCD video camera. The camera allows for digital video to be taken of a specimen mounted on a robotic stage. The stage that the section is mounted on is mobile in XYZ space, with 360 degree sample rotation of the sample mount. Attached to the main stereo microscope is a high-precision, low-eccentricity high torque milling chuck with adjustable speed. Carbide tipped drill bits were used in order to obtain finely powdered carbonate sub-samples. Due to the concentric nature of the growth banding seen in *Acanella* it was important to remain true to the shape of the growth banding in order to decrease the possibility of time averaging, in the event that each distinct growth band represents 2-3 years of growth.

A grid was overlain onto the sample on a LCD monitor to map out the exact location to sample within each growth band. Software coupled with the microsampler allowed for a point-to-point digitization of growth features. The growth features were first digitized in real time as a function of three-dimensional coordinates. To better characterize the growth features, coordinates were interpolated allowing a cubic spline to be fit to the digitized points, while a second spline of digitized points along a growth feature then acts as a guide for which sample paths in between the two splines can be calculated. Intermediate paths were calculated between to digitized paths in order to characterize intervals of the skeleton where banding is not as obvious. Since specimens were hand sanded, the sample surface was not perfectly level. In order to maintain consistent Z depth while sampling, the software allows for sample thickness to be remeasured throughout sampling patterns.

Five sections were prepared for micromilling, a top, middle, and bottom section from the lower part of the colony from A97-1, and a top and bottom section from the lower part of the A97-2 colony. From the sections that were sampled, ~70-96 samples were taken along each transect, totaling 441 samples. Samples were numbered from the outside inward with low numbers indicating material deposited most recently and high numbers indicating older material.

6.3.2 SEM/EDS Sample Preparation

In order to characterize the architecture of growth features within the *Acanella* skeletons, SEM images were taken. Using a LEO 1550 Scanning Electron Microscope at the Center for Environmental Sciences and Technology Management (CESTM), University at Albany, SEM images and corresponding EDS profiles were generated.

Thick sections of both calcite and protein sections were polished on both sides. Resulting sections were ~2-3mm in thickness. Sections were sputter coated with ~200Å (0.02 μm) of either carbon or gold/palladium. Sections and mounting stubs were both coated with silver colloidal paint and left to dry. Once samples were placed on the specimen stage in the sample chamber, both backscatter and secondary electron images were obtained.

6.4 Stable Isotopes

Powdered, micromilled calcium carbonate samples were analyzed at the University at Albany, State University New York stable isotope mass spectrometry laboratory. Each sample was reacted with 100% H_3PO_4 at 90°C in a MultiPrep sample preparation device. The evolved CO_2 gas was then analyzed using a Micromass Optima gas-source triple collector mass spectrometer. All data are reported as per mil deviations relative to Vienna Peedee belemnite (VPDB). The average $\delta^{13}C$ and $\delta^{18}O$ values and standard deviations for 95 samples of standard NBS-19 analyzed during the course of this study were 1.951 ± 0.014‰ and -2.204‰ ±0.026‰ respectively.

Each section of micromilled *Acanella* was analyzed. Some samples were analyzed in duplicate, but the small amount of sample material obtained from micromilling prevented more paired replicates from being analyzed. The samples analyzed are detailed in Table One.

Table I. Number of samples, replicates, and average difference of replicates per section

Acanella Section	# of samples analyzed	# of Replicates	Average Difference of $\delta^{13}C$ between Replicates	Average Difference of $\delta^{18}O$ between Replicates
AB97-1	**93**	**10**	**0.041‰**	**0.040‰**
AM97-1	**97**	**3**	**0.104‰**	**0.087‰**
AT97-1	**92**	**8**	**0.045‰**	**0.056‰**
AB97-2	**89**	**6**	**0.033‰**	**0.049‰**
AT97-2	**70**	**4**	**0.060‰**	**0.041‰**

6.5 Radiocarbon

To attempt to determine the age of the *Acanella* colonies and develop preliminary age models for the $\delta^{13}C$ and $\delta^{18}O$ series samples were measured for $\Delta^{14}C$ using accelerator mass spectrometry (AMS) techniques at the Center for AMS Research at Lawrence Livermore National Laboratory. ^{14}C measurements are reported as $\Delta^{14}C$ values (for age-corrected geochemical samples) according to standard techniques (Stuiver and Polach, 1977). $\Delta^{14}C$ measurements were reported with 1σ total uncertainty of 2.5-3.5‰ (counting statistics and laboratory reproducibility). Material collected for radiocarbon analysis was taken using a hand-held drill from the lower portion of the protein knuckles at the interface between the calcite used for stable isotope analysis and the adjacent protein knuckle. Samples were almost entirely gorgonin. Two samples from A97-1 and two samples from A97-2 were taken from the very outer edge of each coral skeleton representing the year the corals were collected, and from the center of the coral representing the time when the coral began to grow.

Three more radiocarbon samples were taken from AM97-1 from approximately the location that isotope samples 1, 25, and 40 were taken. Samples were taken from these locations in order to provide additional tie points for age model.

Table II. Radiocarbon Results From Middle section of colony #1 (AM97-1):

Sample Name	**$\delta^{13}C$**	**fraction Modern**	**±**	**Δ14C**	**±**	**14C age**	**±**	**Range (year)**
AM97-1 #1 (outside)	-15	0.9450	0.0039	-55.0	3.9	455	35	420-490
AM97-1 #25	-17	0.9414	0.0038	-64.6	3.8	485	35	450-520
AM97-1 #40	-17	0.9415	0.0043	-64.5	4.3	485	40	445-525
AM97-1 #97	-15	0.9143	0.0035	-85.7	3.5	720	35	685-755

Table III. Radiocarbon Results from Top of colony #2 (AT97-2):

Sample Name	**$\delta^{13}C$**	**fraction Modern**	**±**	**Δ14C**	**±**	**14C age**	**±**	**Range (year)**
AT97-2 #1 (outside)	-15	1.1046	0.0043	104.6	4.3	>Modern		
AT97-2 #73	-15	0.9426	0.0038	-57.4	3.8	475	35	440-510

Chapter 7
Results

7.1 SEM

In order to better understand *Acanella* growth and skeletal architecture, a suite of scanning electron microscopy (SEM) images were taken of thick sections of thick sections of coral specimen AM97-1. Initially, one section was prepared from a calcite node. In reflected light, both polished and unpolished thick sections have faint concentric growth bands visible on the surface. The InLens detector used here (Figure 12) allows for very short working distance (distance between specimen plane and the center of the lens). Aside from the faint white halo seen here, no growth features were visible. The calcite node appears very uniform in mineral composition and does not display any variation across the surface. Figure 13 shows the topography inside the central cavity of the *Acanella* stalk more clearly.

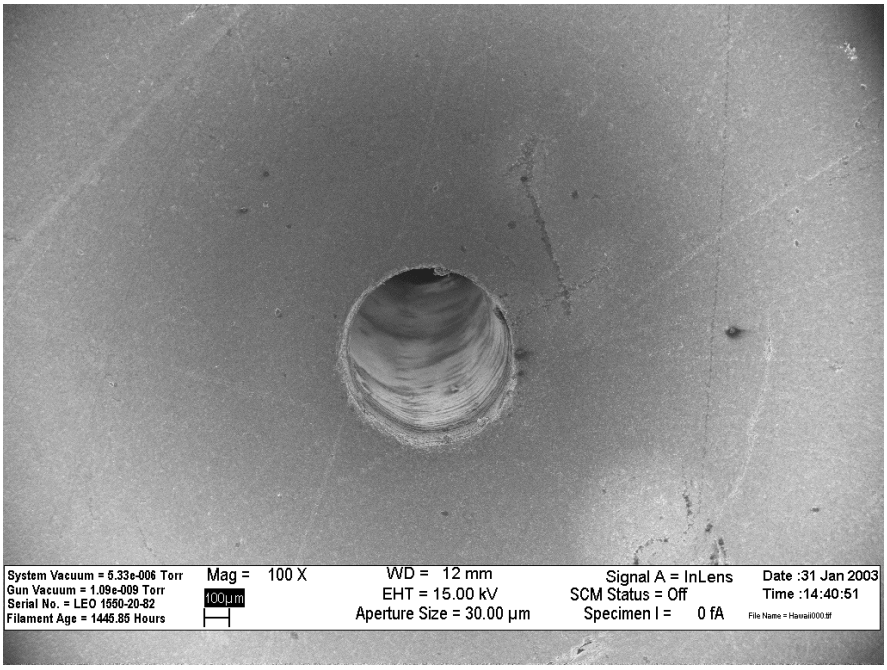

Figure 12. White halo shown at the outer edges of image may be interpreted as a concentric growth feature, one that is composed of lighter colored material possibly due to differences in density. Central cavity in the middle of the specimen shows some evidence of growth banding. Topographical ridges visable on the side of the cavity wall are due to calcite deposition as the coral grows vertically.

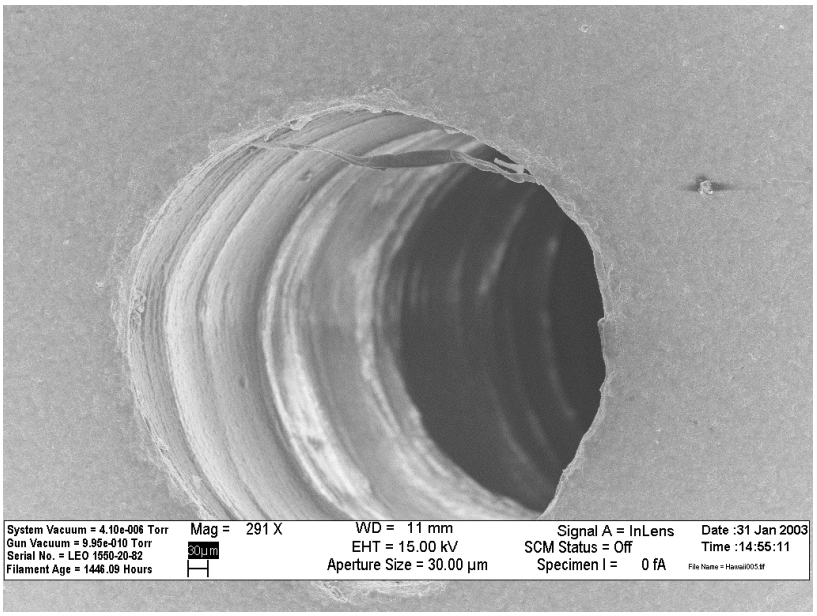

Figure 13. A more detailed image of the *Acanella* central cavity. The contrast between black and white ridges inside the cavity indicates variable topography and density of accreted skeletal carbonate.

Figure 14 shows a cross-sectional view of the same cavity imaged in Figure 13 and illustrates irregularly repeated topographic ridges.

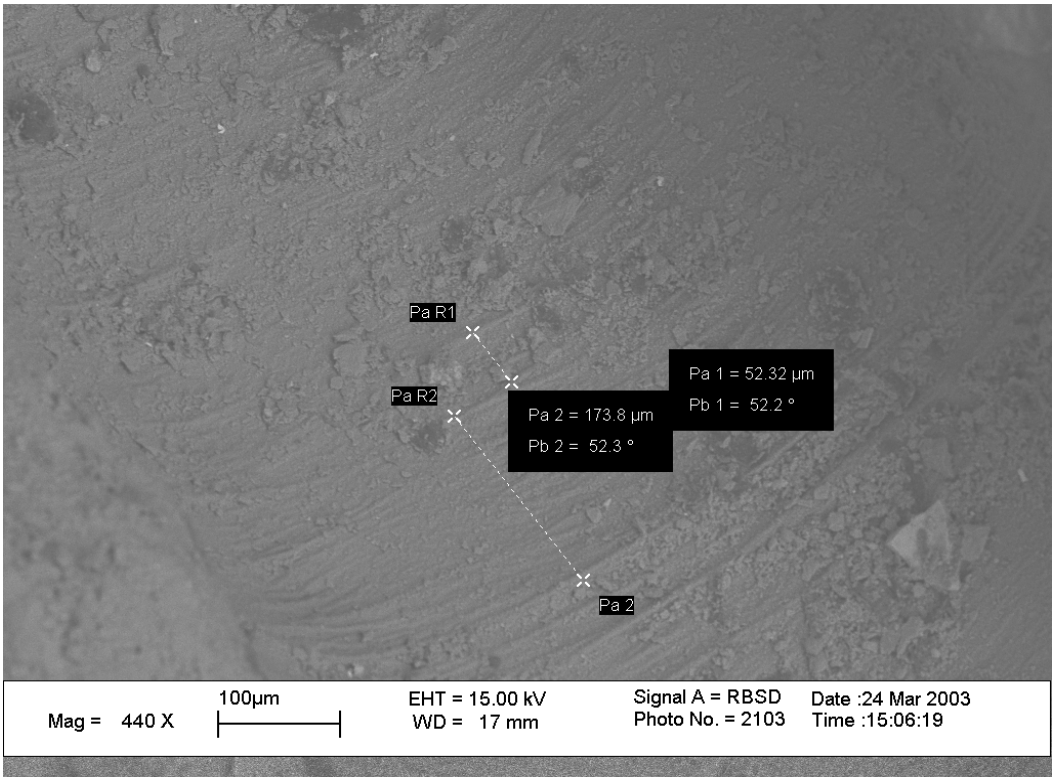

Figure 14. Cross sectional view of central cavity showing varied thickness and length of bands (in µm) along the cavity wall. This image was taken using a Robinson Backscatter Detector (RBSD) in order to image details on the surface of the thick section more accurately.

Figure 15 is an SEM image generated from secondary electrons (SE2) using a standard Everhart Thornley Detector. The solid portion in the upper-left of the image is calcite, and shows weakly distinguishable growth banding. This image was taken specifically from the interface between a calcite node and a gorgonin node (from AM97-1) in order to show how clearly the gorgonin portion shows concentric growth banding (compared to the calcite portion). Note that the horizontal lines and "v" shaped scratches in the upper right of the image are remaining saw marks that survived the polishing

regimen. The more brittle nature of the dried gorgonin is also apparent in this image. Once the coral has been collected and tissue has disassociated, the gorgonin knuckles dry out, shrinking and constricting, but still holding their general shape.

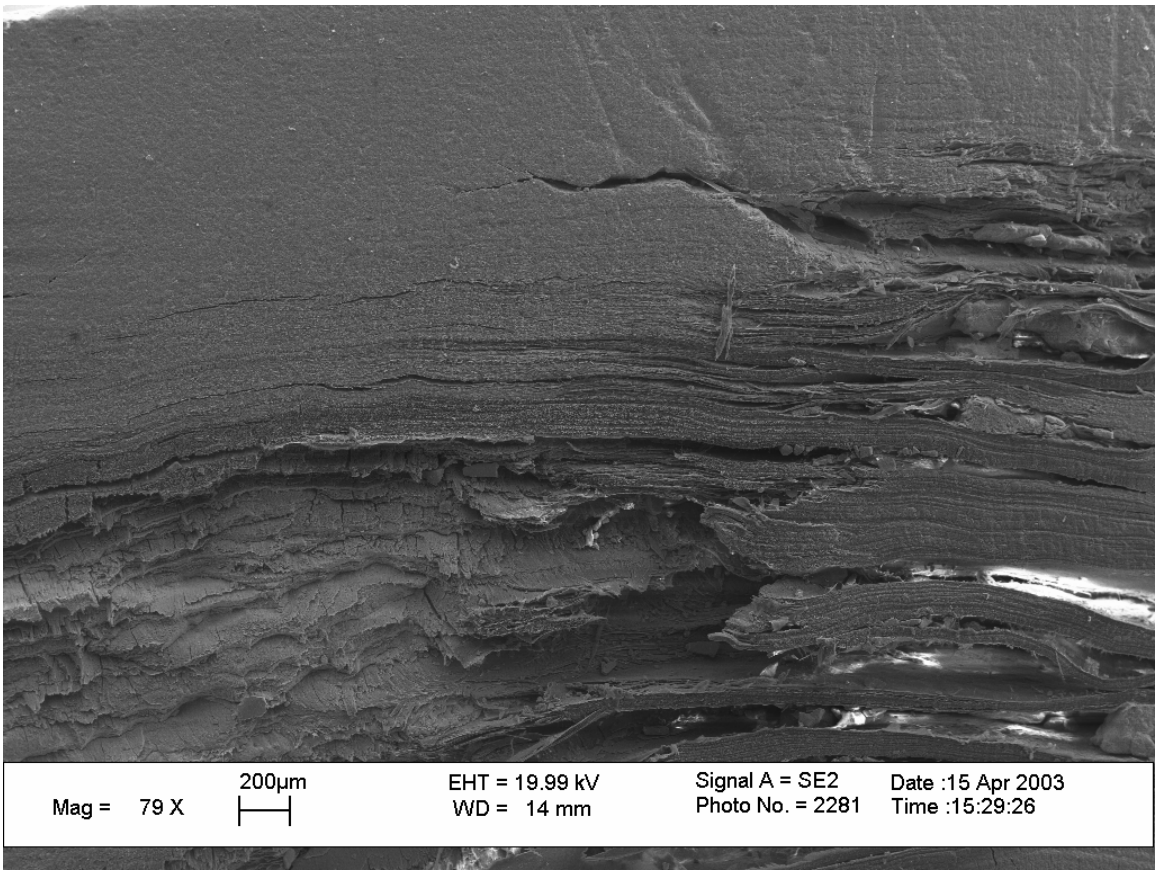

Figure 15. SEM Image shows the difference between calcite and gorgonin. Solid (calcite) material pictured on the upper left side of the specimen does not show obvious growth banding. The other fractured and hackly material is gorgonin, or the same material that *Acanella* "knuckles" are made of.

Figures 16 and 17 (AM97-1) show concentric growth banding in more detail. These images were also taken using a standard Everhart Thornley Detector. Unfortunately, the lowest magnification of this instrument far exceeds the resolution needed to view the entire polished section and to count the concentric growth rings and relate the number of rings to the lifespan that radiocarbon measurements suggest for the *Acanella* studied here (radiocarbon dates to be discussed later). Additionally, compiling a series of images

like the one in Figure 16 in order to account for individual growth bands across the coral specimen requires that the SEM not overlap where the last image was taken. Many more hours of training using the LEO 1550 would be needed in order to successfully manipulate the laser across the surface of the coral accurately imaging growth banding. A rough estimate of the number of growth rings contained in the polished thick section in Figure 17 was calculated from the diameter of the specimen. There are approximately 5-10 growth bands for every 100 μm, yielding between 1500-3000 bands across the diameter of the *Acanella* stalk.

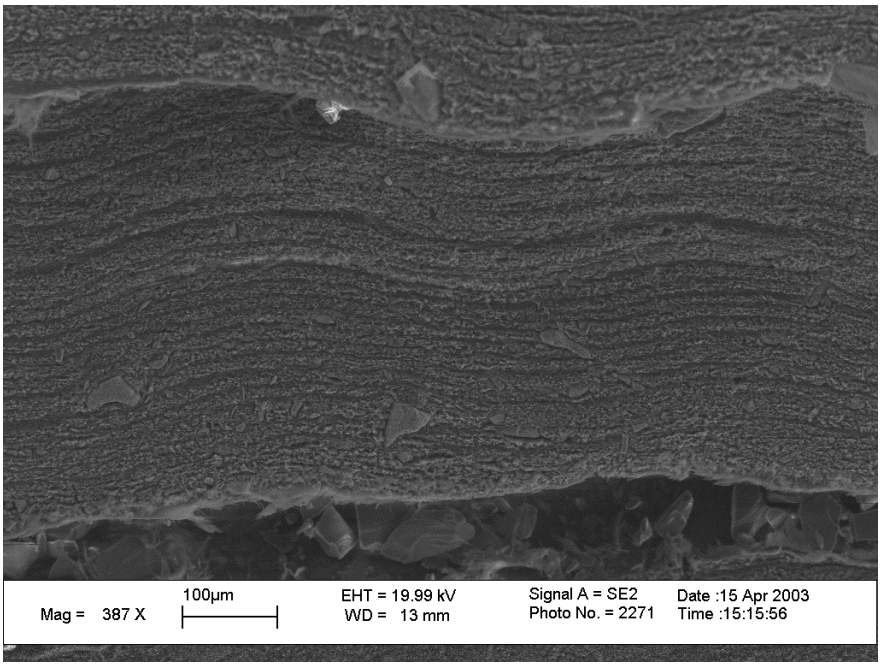

Figure 16. SEM image of concentric growth banding in gorgonin section of *Acanella* Note 100 micron scale.

Figure 17 was taken using a SE2 detector. This image was taken at a much lower magnification (82x) in order to get a better sense of the overlying growth structure of the area in Figure 16 that was magnified by 387x. Figure 16 shows fine growth banding

within four distinct larger concentric features. The cloudy, dark grey area in the lower left corner around which the growth bands have formed is calcite.

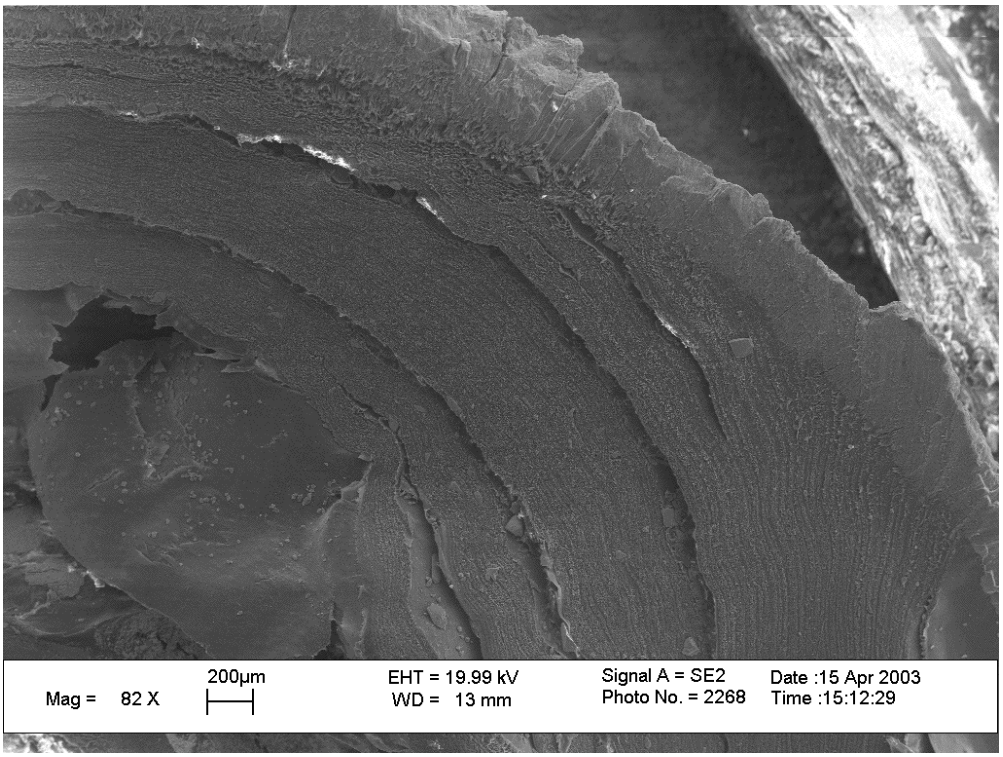

Figure 17. SEM image with lower magnification. Primary and secondary growth features are visible. Note 200 micron scale bar.

The above images are examples from a selection of possible detectors that can be used in SEM imaging depending on specific objectives. For the purposes of this study, the capabilities of the LEO 1550 far exceeded the magnification required. The LEO 1550 is primarily used to image materials down to fractions of nanometers. The SEM was successful in producing highly magnified images that clearly illustrate the character of the growth banding, especially in the protein knuckle portion in *Acanella* Figure 18 indicates that one major and one minor mode of growth band accretion occurs in this

particular specimen of *Acanella*. There are three larger concentric growth bands that are composed of several very subtle concentric growth rings.

The LEO 1550 used for SEM imaging can also be attached to an Electron Dispersive Spectrometer (EDS) that will generate a spectra that shows the number of x-rays collected at each energy, mapping the distribution of elements over an area of interest (Figure 18).

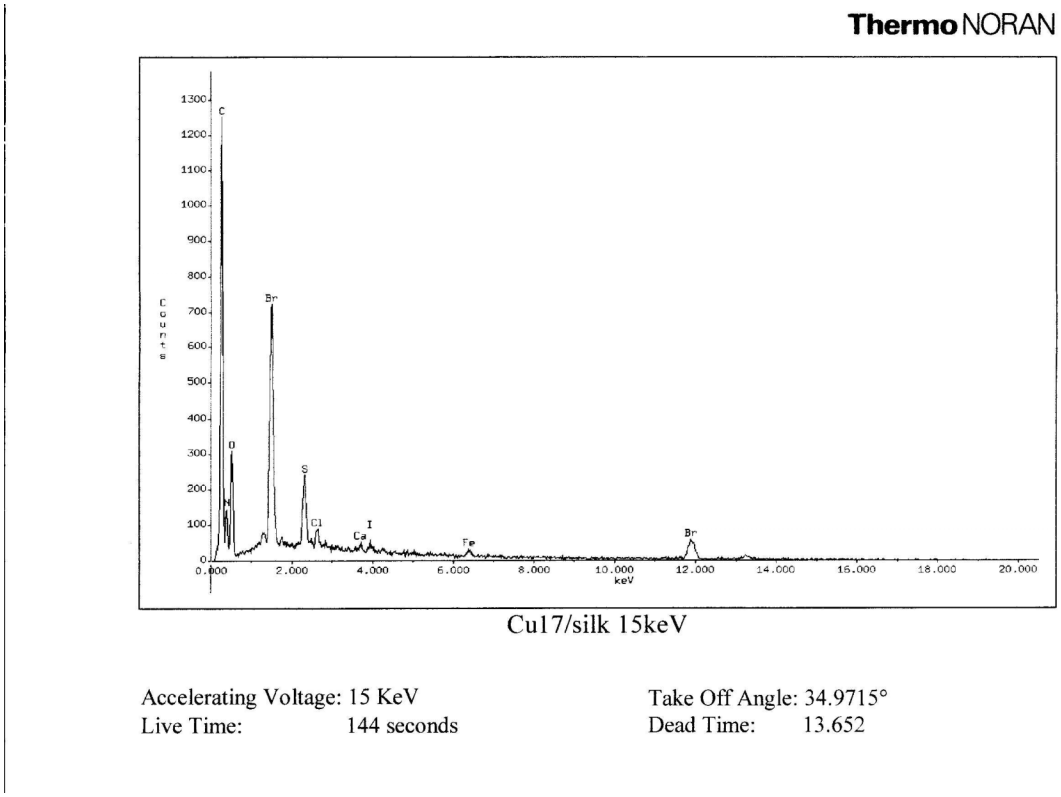

Figure 18. Energy dispersive spectroscopy spectra taken from a transect across AM97-1 gorgonin polished thick section.

During an acquisition of EDS spectra, the laser beam is positioned normal to the sample and rapidly evaluates concentrations of elemental constituents. By scanning the x-ray emission spectra for characteristic x-rays from major elements, it is possible to assign element names to the respective peaks based on the energy of the x-ray signal

generated by a focused electron beam interacting with the specimen surface. The EDS spectrum was generated from the same colony and section (AM97-1) that was imaged in Figures (12-17). Most of the energy outputs are consistent with elements expected to be found in coral gorgonin such as carbon and oxygen. Seawater derived bromine and iodine are also abundant. The Br and I peaks shown in the EDS spectra are representative of normal levels that have been incorporated into the coral skeleton (Nozaki, 1997).

7.2 Radiocarbon Ages

Figure 19 shows the four age dates determined for AM97-1. Data obtained from samples #25 and #40 give the same result of 485 years ^{14}C age. The margin of error increased from ±35 years for sample # 25 to ±40 years for sample #40. The coral was alive when it was collected in 1997. However, time averaging across the outermost section of the coral thick section may have occurred during hand sampling in order to generate enough carbonate material for radiocarbon analysis. Therefore sample #1, or the outermost edge of the coral specimen, corresponds to ~1992. According to the depth-age relationship, the innermost sample, formed when the coral began to grow, dates to AD 1720 ±35 years.

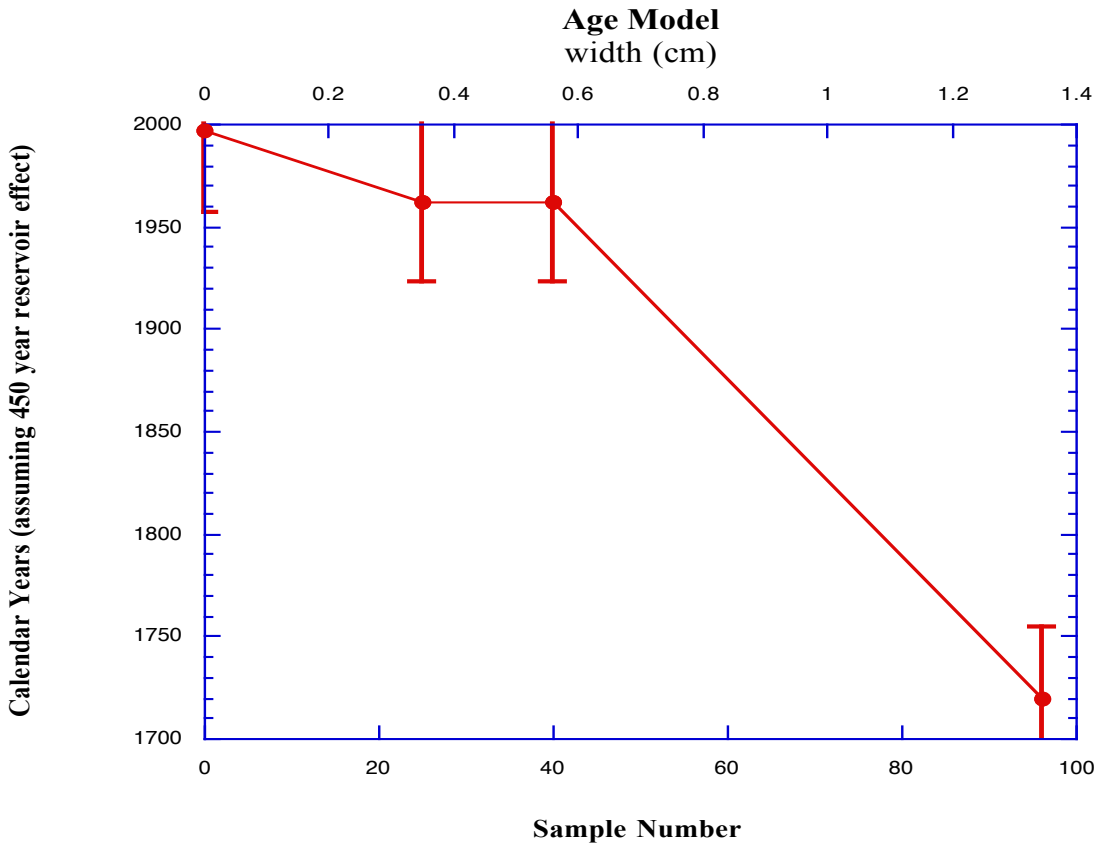

Figure 19. Age Model for specimen AM97-1. Four age dates correspond to samples 1, 25, 40, and 100. Error bars indicate possible errors associated with each sample.

At water depths of 415-440m, there are several corrections that need to be applied to the raw radiocarbon data. One of there corrections is for the reservoir age effect, in order to get the calendar age of a sample. This correction is due to the apparent ^{14}C age of the reservoir from which the coral gets carbon to build its skeleton. Based on the live age of the coral when it was collected and the ^{14}C data, a reservoir correction of 450 years was used so that the specimen's radiocarbon age is consistent with the age of the reservoir in which it formed. Application of a 450 year reservoir correction gives the oldest sample from section AM97-1 an age of ~270 years +/- 35 years. According to Bard (1988), the

reservoir correction in the vicinity (~ 400 m) of the Makapuu Coral Bed is close to 400 years. A reservoir correction of 450 years then is a realistic estimate for a specimen located between 415 and 440 meters of water in the North Pacific.

The section from the second colony, AT97-2, had an inside ^{14}C age of 475 years (Table III), corresponding to a calendar age of ~1970, and a modern age for its outside edge. This colony had samples micromilled from the top and bottom portions of the specimen. Two radiocarbon dates are the only tie-points available for correlating the age model and stable isotope data for Colony 2. The age model that was generated using radiocarbon samples from AT97-2 was used to correlate stable isotope data of AB97-2 as well (Figure 20). The results may imply that smaller solitary corals may grow at a slower rate than larger individuals of *Acanella*. Possible explanations for this could be related to the amount of surface area that an individual coral has exposed to the currents that are delivering the organic particles on which the polyps are feeding. Larger corals would grow at a faster rate compared to smaller/shorter individuals. These results may lead to the conclusion that growth rates are not consistent over the lifespan of *Acanella* nor are growth rates consistent from individual to individual.

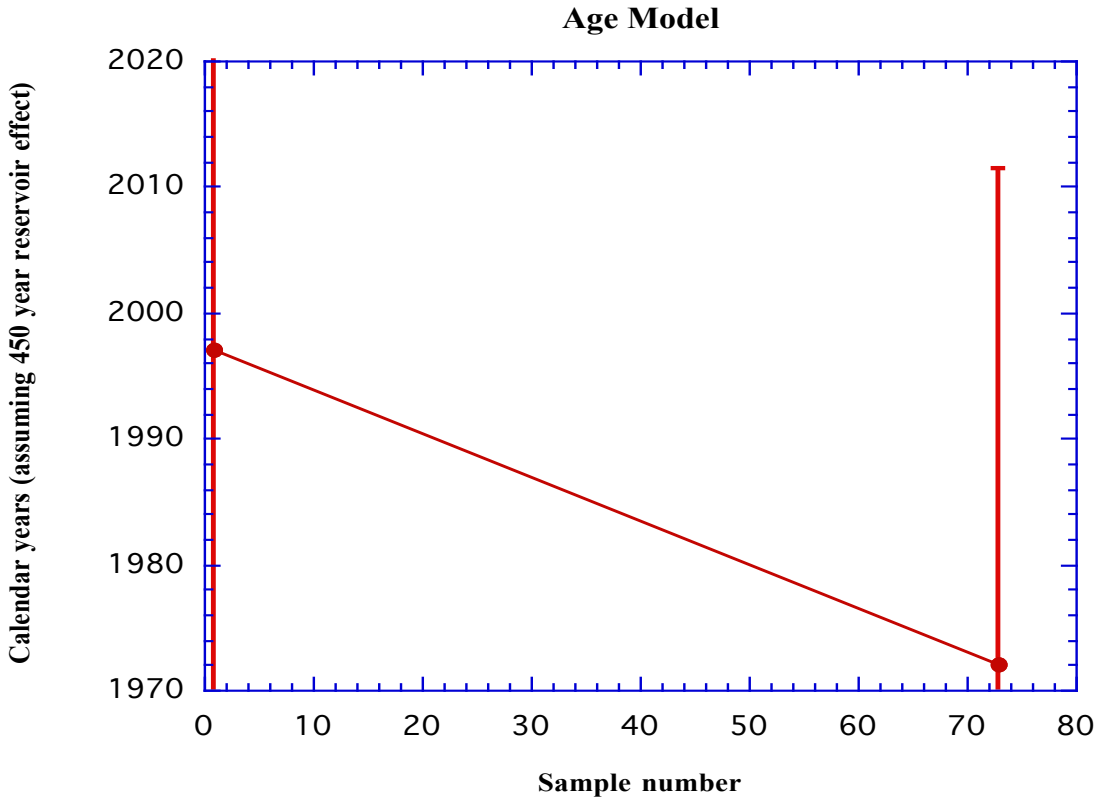

Figure 20. Age Model for second *Acanella* colony AT97-2. Two age dates correspond to samples #1 and #73.

7.3 Stable Isotope Data

7.3.1 Age Model: (AM97-1)

In Figure 21, the same age model that was generated using the radiocarbon data from AM97-1 was applied to AB97-1 and AT97-1. In order to juxtapose the AM97-1 age model generated using Arand software (Howell, 2001) onto the two other sections of the A97-1 *Acanella* colony the same tie points that were used for AM97-1 and the number of samples that were collected from AB97-1 and AT97-1 were plugged into Arand (Ager). The result is three distinct groups of samples all with different quantities

within each thick section of A97-1 (top, middle, bottom) that are plotted using the same age model The innermost sample corresponds to sample #96 and the year 1722 A.D based on the assumptions embedded in radiocarbon data and calendar year calculations (discussed in the Radiocarbon Ages Section). For radiocarbon (and stable isotope) sample #40 (AM97-1), I have assigned the calendar year 1925. This year falls within the range of error associated with this sample and also falls within a best-fit curve of the four radiocarbon samples taken. Sample #25 corresponds to the calendar year 1962, and the outermost sample represents the year that the coral was collected or 1997.

In A97-1, the $\delta^{18}O$ series for the top, middle, and bottom sections of the coral vary only modestly (between 1.1 and 0.4 per mil) and show general agreement (with an offset) until ~1920, at which point all three records exhibit a 0.75 per mil trend towards lower $\delta^{18}O$ until the 1940s, then a 0.5 per mil increase until the mid-1970s, followed by a trend towards lower $\delta^{18}O$ until the outermost sections (youngest) of the skeleton (Figure 21). After 1920, the $\delta^{18}O$ values of the three sections generally coincide, but the amplitude of the $\delta^{18}O$ changes in the bottom section vary only about half as much as the amplitudes of the records of the other two sections.

The $\delta^{13}C$ results in all sections of A97-1 also generally coincide until ~1920 when a large excursion of up to 3‰ to more depleted isotopic values occurs. Once again, the amplitude of this excursion is less pronounced in the bottom sections than it is for the other two sections.

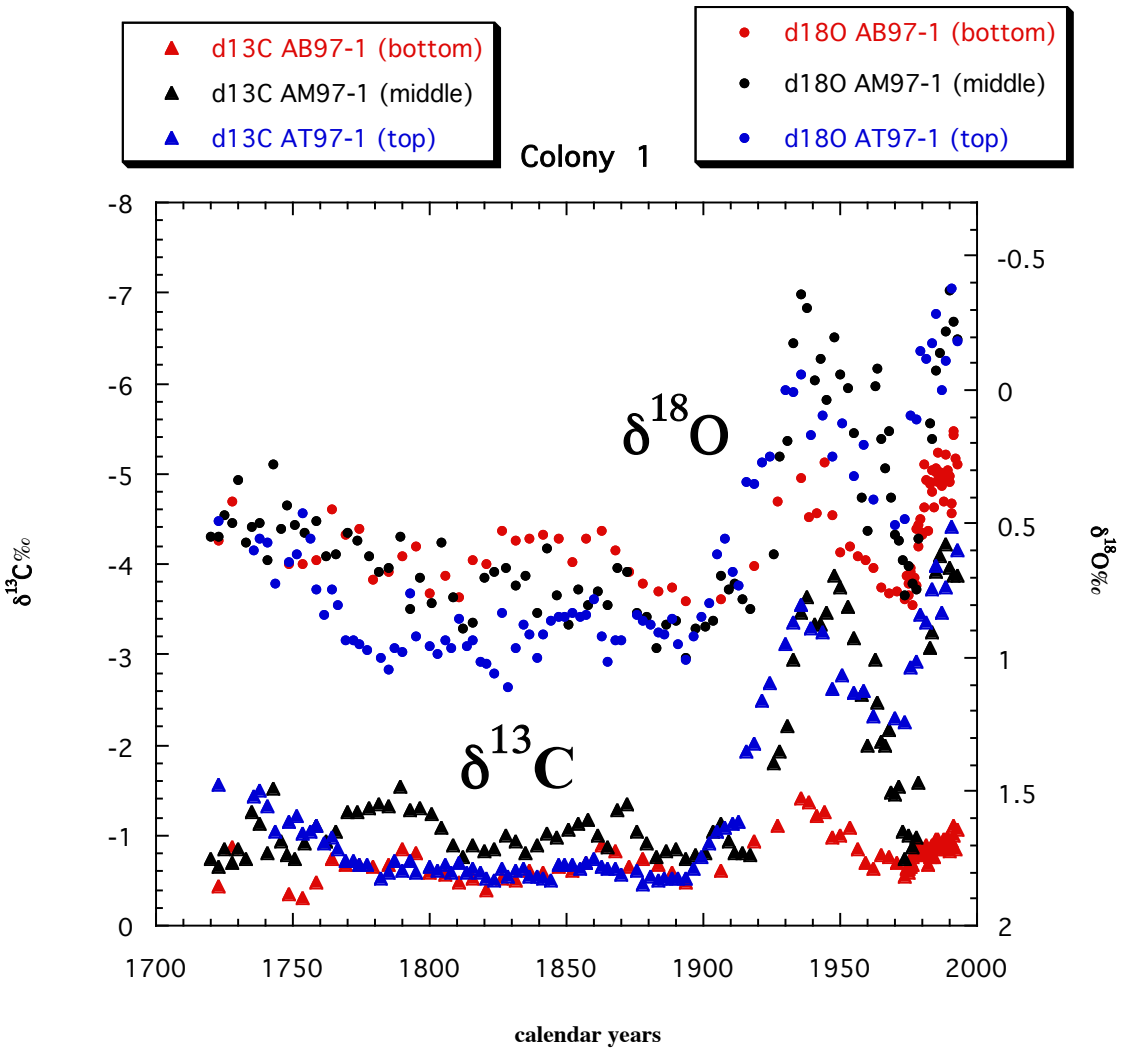

Figure 21. $\delta^{13}C$ and $\delta^{18}O$ values for samples from the top, middle, and bottom of A97-1. Values are given in per mil (‰) vs. VPDB.

7.3.2 Age Model: (AM97-2)

Since the *Acanella* specimen designated as Colony Two was shorter than Colony One prior to thick sectioning, only a top and a bottom section were chosen to sample. In Figure 23, the isotope data from AT97-2 and AB97-2 were plotted against age for Colony 2, based on analyses made from the innermost and outermost samples from AT97-2. It should be noted that about 20 more samples were milled from AB97-2 than from AT97-2. The difference in sampling length is shown in Figure 23, and the discrepancy was

accounted for by applying the same age model generated from AT97-2 radiocarbon age dates. In doing so, the record for AB97-2 (graphically in red) is extended past the actual age date from the inside of AT97-2 by 6 years. Neither the carbon nor the oxygen isotopic composition of Colony two varies as much as they do in A97-1, generally less than 1.0 and 0.5‰ respectively. Despite their reduced amplitudes, AT97-2 and AB97-2 $\delta^{18}O$ data shown are generally coincident between 1975 and 1984 but less so after 1984. On the other hand, the $\delta^{13}C$ data from the top and bottom sections of Colony two do not correspond. AT97-2 $\delta^{13}C$ data show one large excursion occurring at the 1983-1984 interval.

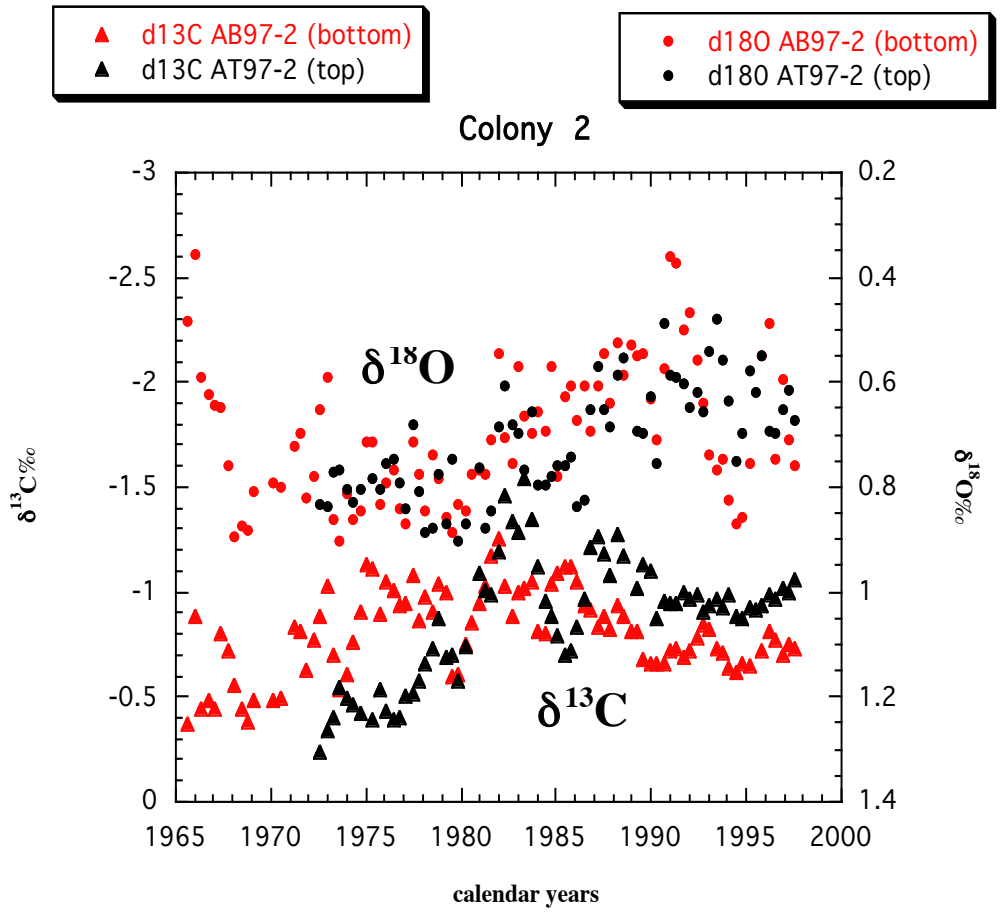

Figure 22. $\delta^{13}C$ and $\delta^{18}O$ values for samples from the top and bottom of A97-2. Values are given in per mil (‰) vs. VPDB.

Chapter 8
Discussion

8.1 Physical Structure of Acanella

The two colonies of *Acanella* studied here, showed patterns of growth banding visible in reflected light and more finely resolved using a SEM. More detailed growth structures were observed in the images of the protein or gorgonin knuckles. Growth bands accrete concentrically around the central cavity in *Acanella*. Some of the rings within the protein knuckle have very thin calcite layers between them. A gorgonin section of A97-2 has 10 distinct growth bands of varying widths that thicken away from the central cavity. Using the SEM, individual growth bands within these larger growth increments were detected (see Figure 17). The larger ring that was imaged using SEM was the outermost ring. In order to make any inferences about how many total bands there were across the whole specimen or the time interval that is represented by each fine band, it would be crucial to image each of the 10 larger growth bands individually, and then sum the bands and compare them with the age of the coral to see if the bands are annual. The magnification capabilities of the LEO 1550 SEM used in this study far exceed what is required to image a ~3 cm in diameter thick section of *Acanella*. The LEO 1550 is most often used in nano-scale imaging of materials. The presence of a finer banding pattern within the larger banding pattern indicates that accretion of these bands is not constant over time, suggesting that the accretion of growth banding could vary based on biological parameters. Possible controls over periodicity and consistency of growth band accretion could be changing environmental parameters in the Makapuu Coral Bed during the lifespan of the coral. As stated earlier, the Makapuu Coral Bed is located in a channel between two Hawaiian Islands. Currents moving through this passage are

considerably stronger than in regions that are more exposed to the open ocean. Currents can cause influxes of sediment to enter the channel supplying increased amounts of particulate organic carbon (POC) to the corals to be incorporated into their skeleton. With a larger supply of sediment, the coral may grow at a more rapid pace than in other times during the coral's life. In contrast, the channel may also become starved of sediment, causing coral growth to slow or even stop. In addition, zooplankton biomass is known to fluctuate with lunar brightness in many parts of the ocean (Hernandez-Leon et al., 2002).

Growth bands can be observed in the calcite portion of *Acanella,* however they were unable to be imaged using the SEM. In reflected light there are 8-10 rings visible in most of the thick section taken from the A97M-1. Unfortunately, because there were no SEM images generated from the calcite portion of the specimen, it is not clear whether the calcite sections have secondary growth features or fine growth bands within the more obvious overlying growth structure. Recently published work by Roark et al. (2005) on growth patterns and lifespans of bamboo corals utilize photomicrographs of carbonate node thin- sections to better characterize growth band geometry and show banding similar to that observed in the gorgonin nodes of AM97-1.

The topography observed within the central cavity of the calcite portion was visible using the SEM (Figures 13 and 14). The combination of the concentric growth rings in both the calcite and the protein sections of the coral stalk and the topography observed in the central cavity indicates that a complex growth achitecture in *Acanella* needs to be understood in order to account for bamboo coral growth geometry, both in height and in diameter of the coral stalk. Colonies of *Acanella* have the largest stalk

diameter closest to the base of the stalk. The stalks are much smaller in diameter towards the outer extremities of the coral's colony (see Figure 8).

Images of finely banded gorgonin nodes seen in Figures 14, 15, 16, and 17 show that the coral is laying down thin layers of skeletal material in order to grow both stalk diameter and vertically. Still, it is unknown how the veneers are deposited with respect to time and how vertical/linear growth relates to the deposition of the concentric growth bands. In order to account for growth of the coral in both directions, *Acanella* must be simultaneously depositing thin veneers of calcite and gorgonin. In future work, the coral should be age dated with higher resolution ^{14}C across the diameter of the specimen. Additionally, if it were possible to preserve the original orientation of the coral colony once the coral was collected and after the knuckles disassociate from the calcite nodes, the smallest outer extremities of the coral branches, as well as the basal growth plate of the coral colony should be dated. Only then can a more complete assessment of general *Acanella* growth geometry be made. Developing a better understanding of the growth architecture of *Acanella* is essential before it can potentially be used as a paleoceanographic archive.

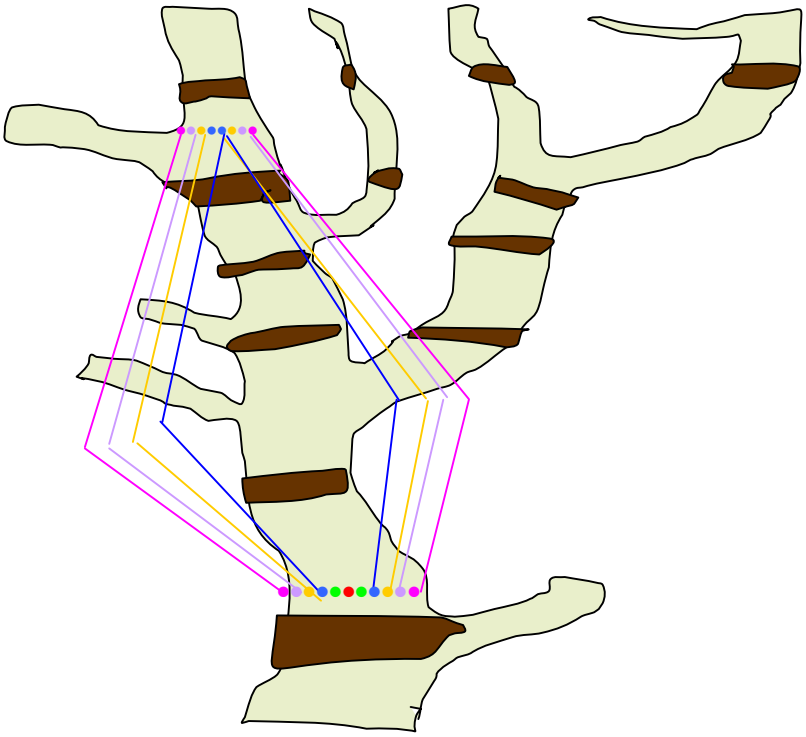

Figure 23. Schematic of coral growth geometry accounting for growth both vertically and horizontally from central chamber. Color-coded dots indicate relative ages of coral as the colony gets taller.

Figure 23 is a schematic representation of relative age throughout the whole colony. Samples dated in this study were taken from sections of the coral with the widest diameter. A more comprehensive study would date the coral at varying heights in the colony in order to indicate the growth and skeletal extension rates.

The red lines in Figure 24 indicate that the calcite sections and the gorgonin knuckles are in near-horizontal alignment across the whole colony, suggesting that the calcite and protienaceous nodes may be deposited simultaneously. Thus, it may be

possible in the future to use gorgonin knuckle position as a stratigraphic marker within an *Acanella* colony.

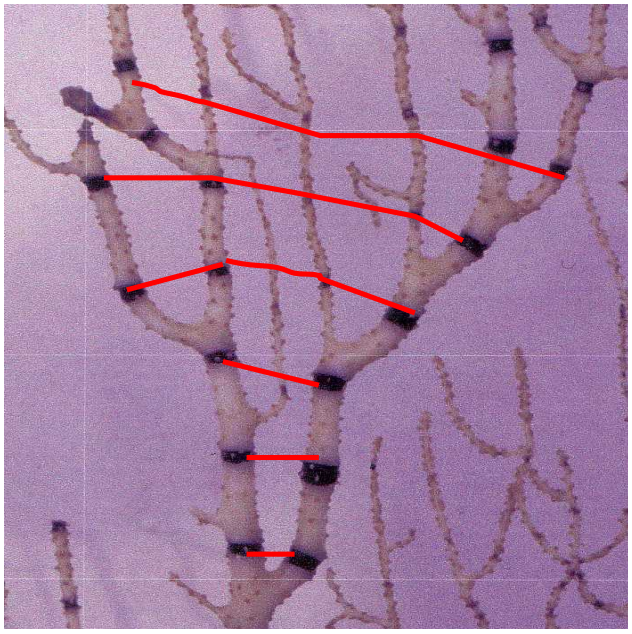

Figure 24. Digital photo taken of *Acanella* during collection phase. Red bars have been superimposed over image to point out gorgonin knuckle horizons.

8.2 Sources of carbon to deep sea corals

Two of the sources of anthropogenic carbon in the atmosphere are thermonuclear bomb testing and the burning of fossil fuels. Testing of thermonuclear weapons in the 1950's caused an increase in the production of radiocarbon in the atmosphere, while burning of fossil fuels has diluted the ^{14}C content of the atmosphere by the injection of the ^{14}C-free CO_2 formed since last century by the combustion of old-carbon. Unfortunately, more ^{14}C data points are needed in order to determine if the Suess Effect has been recorded by the corals studied here. The presence of bomb carbon in *Acanella* samples at 420m indicates that the same mechanism of vertical mixing that transports

salinity maxima from the surface to the main thermocline is also transporting anthropogenic carbon.

8.3 Skeletal Growth

Karl et al. (1996) defines the "biological pump" as the collection of different mechanisms that diffuse and advect dissolved inorganic and organic particles into the subeuphotic zone from the surface photic zone. For the protienaceous portion of the skeletons of *Acanella,* the carbon is being derived from the organic carbon pool, possibly from surface-derived particulate organic carbon (POC), sedimentary organic carbon (SOC), and/or dissolved organic carbon (DOC) (Druffel et al., 1995). Letelier et al., (2000) pinpoint a strong North Pacific Gyre upwelling event in March and April of 1997. The study used data recorded at the ALOHA station showing an increase in dissolved organic matter and a displacement of the thermocline by 120 m. Researchers concluded that this large upwelling event (and resultant themocline shift) was probably the result of a strong wind divergence and/or the passage of a cyclonic eddy through the HOT/ALOHA study area. Most likely POC is the greatest contribution in gorgonin formation. POC is generated in the euphotic zone, and then either sinks or stays suspended in the water column. The presence of bomb radiocarbon in the outer layers of the *Acanella* skeleton studied here is further evidence that supports POC contributing to this portion of the coral skeleton is. The organic portion of *Acanella* may record surface water chemistry while the calcite sections record the conditions in the depth range where the corals grew. Druffel et al. (1995) suggested that $\delta^{13}C$ similarity between layers could indicate that there were not large changes in POC flux over time. They analyzed the $\delta^{13}C$ value of the deep sea-coral *Gerardia* at various heights in the coral colony. Analyses

made from the trunk, branch, and base of the coral *Gerardia* varied minimally, suggesting that fractionation occurring during the uptake of carbon by deep-sea corals during their lifespan remained constant. Results seen in *Acanella* $\delta^{13}C$ data (Figure 21) suggest that surface water CO_2 concentrations vary enough to account for a 2 per mil change in the $\delta^{13}C$ after approximately 1920.

Other explanations for gorgonin knuckle alignment might be the result of a regular cycling of POC at this depth. In this instance, comparison of ages from the smaller extremities and the basal growth plate would be useful to check the validity of different ages at different heights in the coral. Alternatively, if accretion of gorgonin knuckles is occurring simultaneously, then consistent POC levels would need to be maintained at ~400 m depths where the coral grew. It is also possible that *Acanella* has some other biological mechanism at work that has spaced gorgonin knuckles out almost perfectly throughout the colony. Profile data stored in the HOTs data repository show that between 400 and 500 m between 1989 and 1997 particulate carbon flux varies between 55 and 15 mmol/m^2. The greatest interval of change is seen between 1994 and 1996. At this point it is unknown what the exact cause of the alternating segments of gorgonin and calcite in *Acanella* is. Further unraveling of coral skeleton geometry in order to study growth architecture is needed to make more detailed deductions about *Acanella* growth pattern architecture.

8.4 $\delta^{18}O$ vs. $\delta^{13}C$ Equilibrium

Understanding the offset or "vital effect" of the isotopic equilibrium for various carbonate species continues to complicate the study of paleoclimates. The study of isotopic equilibrium in deep-sea corals is simplified by their lack of algal symbionts,

coupled with the relatively constant temperature, salinity, and isotopic composition of the waters that deep-sea corals live in. (McConnaughey 1989a).

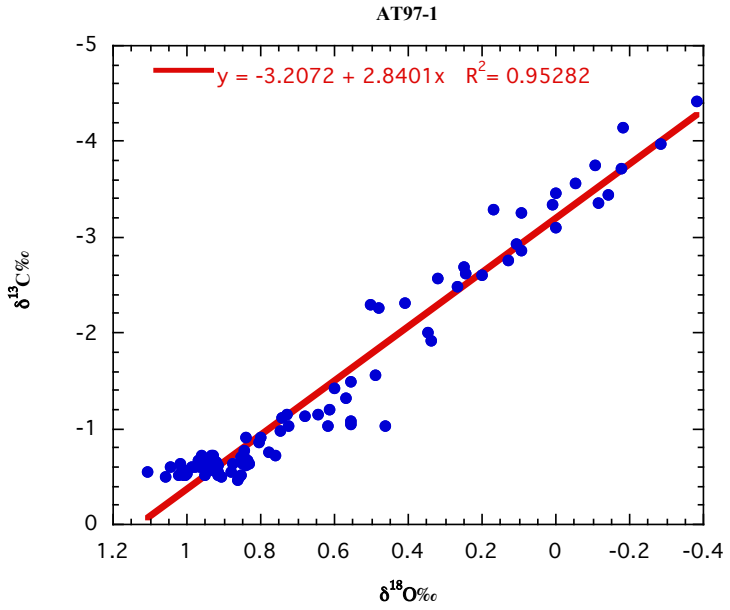

Figure 25. $\delta^{13}C$ vs. $\delta^{18}O$ AT97-1. These samples are from the top of the section that was analyzed from colony one. $R^2 = 0.95$.

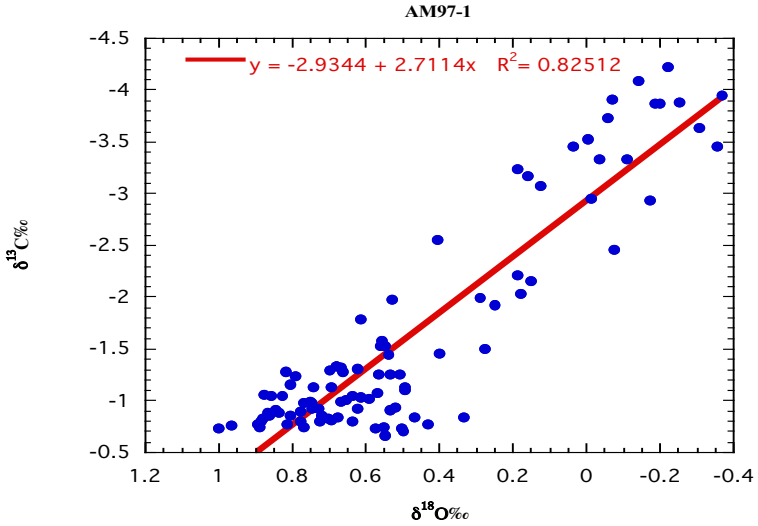

Figure 26. $\delta^{13}C$ vs. $\delta^{18}O$ AM97-1. These samples are from the middle of the section that was analyzed from colony one. $R^2 = 0.83$.

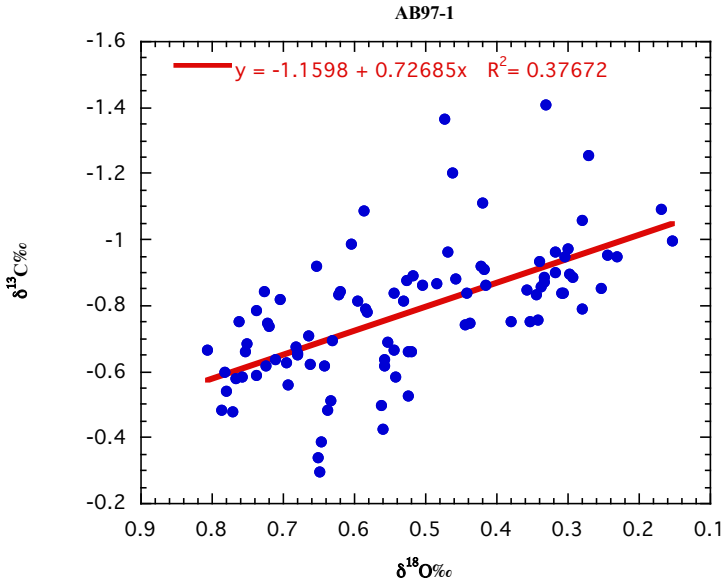

Figure 27. $\delta^{13}C$ vs. $\delta^{18}O$ AB97-1. These samples are from the bottom of the section that was analyzed from colony one. $R^2 = 0.38$.

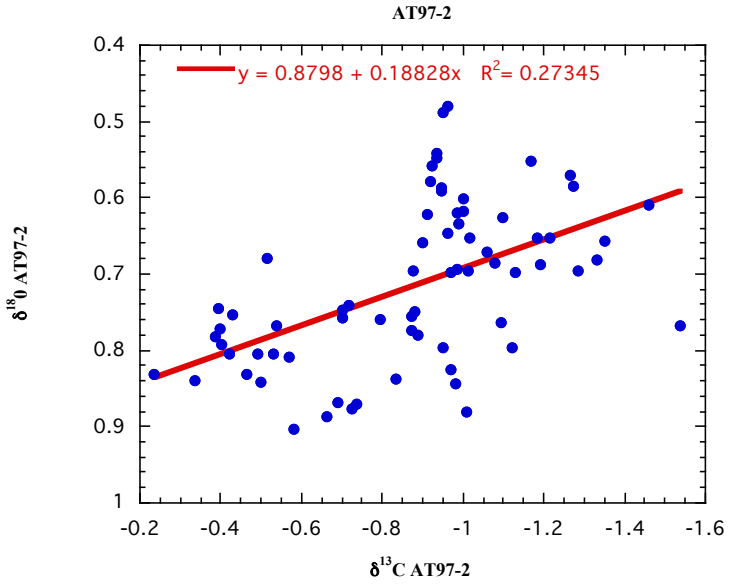

Figure 28. $\delta^{13}C$ vs. $\delta^{18}O$ AT97-2. These samples are from the top of the section that was analyzed from colony two. $R^2 = 0.27$.

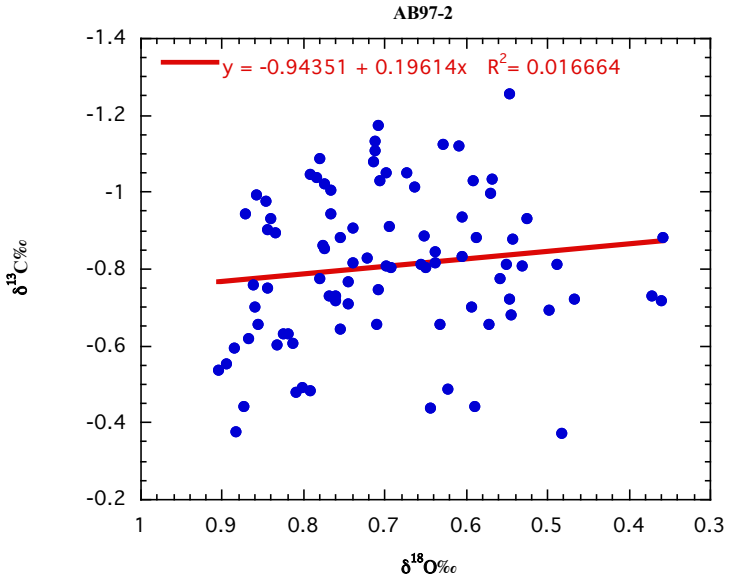

Figure 29. $\delta^{13}C$ vs. $\delta^{18}O$ AB97-2. These samples are from the bottom of the section that was analyzed from colony two. $R^2 = 0.02$.

The fractionation of C and O isotopes during the process of carbonate skeleton building is considered to be in part kinetic affected by slower reaction rates during CO_2 hydration and hydroxylation (McConnaughey, 1989b; McConnaughey, 2003). Adkins et al. (2003) extended McConnaughey's research of carbonate and kinectic models of isotopic (dis)equilibrium in ahermatypic, non-photosynthetic corals to account for the effect of ambient pH on skeletogenesis. During calcite precipitation under equilibrium conditions, calcite is enriched by ~1‰ over the bicarbonate in solution. Rapid calcification of biological carbonates is associated with strong disequilibrium (Figures 28 and 29), whereas a demonstrated linear relationship between $\delta^{13}C$ and $\delta^{18}O$ (Figures 25 and 26) assumes that CO_2 hydration and hydroxylation proceeded slowly.

The r^2 values of the top, middle, and bottom sections of A97-1 of *Acanella* are 0.95, 0.82, and 0.37 respectively, and for A97-2 the r^2 for the top section is 0.27 and 0.01 in the bottom section. Since the physical properties of the ambient seawater in the Makapuu Coral Bed go relatively unchanged and photosynthesis is not affecting the surrounding carbon pool, it is possible that varying isotopic signatures among the *Acanella* thick sections studied here is the result of varying calcification site chemistry. It is thought that pH at the calcification site may cause such variation between species and even sub-samples of the same species (Adkins et al. 2003). There is no body of research that explores how to sample the very thin membrane across which calcification takes place. Understanding more about *Acanella* growth patterns may also help to determine the cause for such variable vital effects with one species of deep-sea coral.

8.5 Stable Isotopes

In A97-1 the variations in the $\delta^{13}C$ and $\delta^{18}O$ in the bottom, middle, and top sections generally coincide, although the amplitude of variations of both $\delta^{13}C$ and $\delta^{18}O$ are significantly attenuated in the internal (older) samples. This suggests that any change in the carbon pool, water chemistry, and/or water temperature affected all sections but that the muted response measured in the older portion may be due to some aspect of *Acanella* growth, or to an environmental change. Controls on skeletal $\delta^{13}C$ include the isotopic composition of seawater and the growth rate of the coral (Miller, 1995). The $\delta^{13}C$ of seawater is controlled by the balance between primary production, degradation of organic C in the water column, and air-sea exchange.

Because these *Acanella* lived in the permanent thermocline in Hawaii, the variability in water temperature should be minimal. However, large subsurface anomalies occur in the North Pacific in the mid-1970's. This change is thought to have been a major climate regime shift (Nitta and Yamada, 1989; Trenbreth, 1990). As a result of this regime shift and changes in the subsurface, SST decreased by 1° in the central and western North Pacific while SST warmed by 1°along the west coast of the U.S. (Deser, 1996). According to Deser's (1996) findings, interdecadal variations are most prominent below 150 m in the central North Pacific, while changes along the west coast of North America appear to be confined to 200-250 m. Others, such as Talley and White (1987) and Antonov (1993), note a cooling trend starting as early as 1957 and lasting through 1984. The cold masses originated at the surface and propagated to the main thermocline at ~ 100 m/yr^{-1}. This propagation of cool water masses shifted the

position of the main thermocline accounting for at least some of the $\delta^{18}O$ variability measured in *Acanella*.

In shallow water, light penetration into and clarity of the water column could contribute to hermatypic skeletal $\delta^{13}C$ variability (Dunbar and Cole, 1990). For example if there are any photosynthesizing corals in the vicinity of azooanthellar corals, then the carbon pool will presumably become in enriched in ^{13}C as zooxanthelate corals preferentially fix ^{12}C (McConnaughey, 1989a). Deep-sea coral such as *Acanella*, McConnaughey's findings suggest, will respond to the pH gradient in the coral's calcification system, ultimately determining calcification rates. Using this theory, high pH levels would cause high rates of calcification and cause negative $\delta^{13}C$ values (Swart et al., 2005). HOTs data show that pH levels between 400 and 500 m of water measured at the ALOHA(2) station from 1992-1997 range between 7.798 and 7.491. Even though pH only varies on the order of ~ 0.2 for this 100 meter section of the thermocline, pH at the calcification site might be more variable, accounting for changes in growth rate from one solitary deep-sea coral to the next.

The hydrologic balance between precipitation, evaporation, and advection of water masses influences the $\delta^{18}O$ composition of seawater. If the $\delta^{18}O$ biogenic calcium carbonate is solely a function of temperature, then the $\delta^{18}O$ of biogenic calcium carbonates would have decreased by about 0.22‰ for every 1°C rise in water temperature (Epstien et al., 1953). Assuming the developed age model approximates the correct age model, between ~1920 and ~1940 there was a pronounced depletion of ^{18}O, the largest of which appears in the $\delta^{18}O$ record of AM97-1 (middle section). During this time there is an average $\delta^{18}O$ shift of ~0.7‰. Using the Epstien et al., (1953) temperature-$\delta^{18}O$

relationship and assuming that the entire change was due to temperature, this 1.35‰ $\delta^{18}O$ change would suggest that water at 400 m warmed by almost 6° over ~ 20 years. Shifting the thermocline 50 meters in either direction would cause the thermocline to respond with a 2° temperature change. Based on preliminary observations, the thermocline would have shifted anywhere between ~100-120 m. Another pronounced depletion in ^{18}O between about 1975 and 1990 indicates a water temperature increase of 5° during a ~15 year time period. Both of these excursions are exhibited in the AB97-1 and AT97-1 records, but with smaller amplitudes (see Figure 21). Despite limitations of the age model developed for A97-1, the timing of the changes in $\delta^{18}O$ are remarkably close to positive and negative phase changes of the PDO in this region. The $\delta^{18}O$ data presented in this pilot study (assuming a correct age model) provide convincing support for the use of *Acanella* as archives of paleoceanographic properties.

There is a salinity minimum found in the North Pacific Intermediate Waters. At the ALOHA station water has been affected by saline intrusions ranging between 5 and 100m in thickness at depths between 350 and 1000m of water. It is possible that the variations seen in the $\delta^{18}O$ record are a response to hot and dry conditions that persist during El Nino years. For example, severe drought occurred in Hawaii during the El Nino years 1997-1998. During these dry conditions, surface evaporation leads to increased sea surface salinity causing enrichment of ^{18}O in surface seawater.

Although I acknowledge that the age model for A97-2 is poorly constrained, if we assume it is correct, then the $\delta^{18}O$ and $\delta^{13}C$ variations recorded in this colony (Figure 24) show few similarities to those measured in A97-1 except for the depletion in ^{13}C between 1975 and 1985 and the depletion in ^{18}O between 1980 and 1990. There are two

features in the $\delta^{18}O$ record of AB97-2 that could represent a temperature change of ~ 2° C from 1965-1967 and 1990-1995. Compared to the changes seen in colony one, the isotopic variability in colony two occurs on shorter time scales and with smaller amplitudes. At first glance, it seems likely that two specimens of the same species of coral, collected within 20 m each other during the same dive would have similar $\delta^{18}O$ and $\delta^{13}C$ temporal patterns. However, as stated by Grigg (1974) it is possible that two deep, solitary corals located in even closer proximity than 20 m of water, have the potential to have widely varying growth rates. Grigg (1974) attributes changes between colonies of solitary corals as close as three meters apart to be related to small differences in food supply or other differences in microhabitat.

Chapter 9

Conclusions and Recommendations for Future Work

Based on the results of this pilot study, it is apparent that in order to prove that *Acanella* is a good paleoceanographic archive more data are needed. Future work may include additional radiocarbon dating or other dating methods (eg., ^{210}Pb or Ur/Th) to provide support for the existing age model presented here. A more extensive age model would help shed light on whether the discrepancy in age models between the two *Acanella* colonies is real, ultimately validating the Grigg (1974) assertion that corals as close as 3m apart can have widely varying geochemistries based on their distinctive microhabitat. Selection of coral skeleton sub-samples should be collected from various places across the entire colony, not just towards the base of the colony as was done here. In order to best represent the age of the colony, it is necessary to date the coral across the diameter of the stalk after the methods used in this study. In addition to the samples collected across a radial transect of the coral base, I would also date material from the smaller branching arms of the coral in order to decipher whether or not the coral is depositing calcite and gorgonin simultaneously, or whether they extend their skeleton from the base of the skeleton only. If there is enough material, there should be a set of ^{230}Th dates using the same material that was radiocarbon dated. The combination of these dating methods could strongly constrain changes in cosmogenic nuclide production rate and changes in carbon between active reservoirs (Adkins, 2002). Further, once more is understood about bamboo coral growth patterns a study of linear growth rates would be useful. Monitoring linear growth rates would provide information on the overall growth

geometry of the coral as well as indicate differences in growth patterns and lifespan from one solitary coral to the next.

Based on the fact that the two solitary corals situated in close proximity to each other studied here do not resemble each other in age or isotopically, future work on *Acanella* should include more than two colonies in order to infer some semblance of how this species responds to ambient changes in the main thermocline. It is obvious between the two colonies of solitary *Acanella* studied here that valuable oceanographic information is being archived in the coral's skeleton throughout its lifespan. Perhaps a more in depth investigation in future studies of solitary deep-sea corals would include the chemical and biological aspects of each coral's microhabitat that would cause corals as close as 20 m apart to develop so differently.

At this point we can say nothing about what degree of periodicity or seasonality the growth rings seen in both the calcite and gorgonin nodes are accreting. We are able to note through high-resolution SEM images that there are very fine bands of gorgonin which may be representative of annual banding. Approximations made based on the amount of growth bands counted might imply that growth increments are annual. However, in order to accurately do this, all of the major growth bands must be imaged in detail to get an exact count of growth bands.

$\delta^{18}O$ data collected from A97-1 are unmistakably synchronous with two major regime shifts seen in the PDO. Major shifts occur at 1940 and 1976 in both the isotopic data presented in this pilot study and in the Mantua (1997) PDO record. Therefore, it may be inferred that *Acanella* is recording phase changes of the PDO between 400 and 500 m where *Acanella* was collected. By inference I have determined that the

temperature changes indicated in A97-1 are related to changes in thermocline depth (due to phase changes in the PDO) that have occurred during the *Acanella* lifespan. They show that *Acanella* is in fact recording and archiving paleoceanographic properties. However, interpretations of paleoceanography and paleoclimates in future research of solitary deep-sea bamboo corals needs to be coupled with an extensive analysis of growth patterns and coral skeleton architecture. More information regarding the *Acanella* growth geometry will guide a more accurate radiocarbon and isotopic sampling regimen. More extensive sampling of colony two might reveal similar findings to that of colony one. Conversely, a more extensive sample set might further confirm Grigg (1974) findings that indicate varying results from specimen to specimen.

References Cited

Adkins, J.F., Boyle, E.A., Cheng, H., Druffel, E.R.M., Edwards, R.L. 1998. Deep-sea coral evidence for rapid change in ventilation of the deep North Atlantic 15,400 years ago. Science. 280(5346). 725-728.

Adkins, J.F., Griffin, S., Kashgarian, M., Cheng, H., Druffel, E. R. M., Boyle, E. A., Edwards, L. E., Shen, C. 2002. Radiocarbon Dating of Deep-sea corals. 44(2): 567-580.

Adkins, J.F., Boyle, E.A., Curry, W.B., Lutringer A. 2003. Stable Isotopes in deep-sea corals and a new mechanism for "vital effects". Geochimica et Cosmochimica Acta. 67(6). 1129-1143.

Alexander, M.A. 2003. The impact of ENSO on the North Pacific Ocean-Atmosphere System During Summer. 13th Conference on the Interactions of the Sea and Atmosphere.http://ams.confex.com/ams/BLTAIRSE/techprogram/paper_77915.htm.

Antonov, J.I. 2005. Linear trends of temperature at intermediate and deep layers of the North Atlantic and the North Pacific oceans: 1957-1981. Journal of Climate. 6(10). 1928-1942.

Auad, G., Kennett, J.P., Miller, A.J. 2003. North Pacific Intermediate Water response to a modern climate warming shift. Journal of Geophysical Research. 108(C11): 131 -138.

Bard, E. 1988. Correction of Accelerator mass spectrometry 14C ages measured in planktonic foraminifera: paleocenographic implications. Paleoceanography. 3(6): 635-645.

Bingham, F.M., Lukas, R. 1996. Seasonal cycles of temperature, salinity, and dissolved oxygen observed in the Hawaiian Ocean Time-Series. Deep-Sea Research II. 43, no 2-3: 199-213.

Deser, C., Alexander, M.A., Timlin, M.S. 1996. Upper-Ocean Thermal variations in the North Pacific during 1970-1991. 9: 1840-1855.

Druffel, E.R.M., Benavides, L.M. 1986. Input of excess CO_2 to the surface ocean based on $^{13}C/^{12}C$ ratios in a banded Jamaican sclerosponge. Nature. 321(6065). 58-61.

Druffel, E.R.M., King, L.L., Belastock, R.A., Buesseler, K.O. 1990. Growth rate of a deep-sea coral using ^{210}Pb and other isotopes. *Geochimica et Cosmochimica Acta*.54: 1493-1500.

Druffel, E. R. M., Griffin, S., Witter, A., Nelson, E., Southon, J., Kashgarian, M., J, Vogel. 1995. *Gerardia*: Bristlecone pine of the deep sea? Geochemica et Cosmochimica Acta. 59(23): 5031-5036.

Druffel, E. R. M., Griffin, S., Guilderson, T.P., Kashgarian, M., Southon, J., Schrag, D.P. 2001. Changes of subtropical North Pacific radiocarbon and correlation with Climate variability. Radiocarbon 43(1): 15-25.

Dunbar, R.B., Cole, J.E., 1990. Coral Records of Ocean – Atmosphere Variability. NOAA Climate and Global Change Program. Special report no. 10.

Epstein, S., Buchsbaum, R., Lowenstam, H.A., Urey, H.C. 1953. Revised carbonate-water isotopic temperature scale. Bulletin of the Geological Society of America, 64. 1315-1326.

Federov, A.V., Philander, S.G. 2000. Is El Nino changing? Science. 288(5473). 1997-2000.

Folland, C. K., Mullan, A.B., Renwick, J.A., Salinger, M.J. 2002. Relative influences of the Interdecadal Pacific Pacific Oscillation and ENSO on the South pacific Convergence Zone. Geophysical Research Letters 29, 21-24.

Griffin, S., Druffel, E. R. M. 1989. Sources of Carbon to deep-sea corals. Radiocarbon, 31(3): 533-543.

Grigg, R.W. 1974. Growth rings: Annual periodicity in two Gorgonian Corals. Ecology, 55. 876-881.

Grigg, R.W. 1988. Recruitment limitation of a deep benthic hard-bottom octocoral population in the Hawaiian Islands. Mar. Ecol.Prog. Ser 45: 121-126.

Grigg, R.W. 1993. Precious Coral Fisheries of Hawaii and the U.S. Pacific Islands. Marine Fisheries Review 52(2): 50-60.

Grigg, R.W. 1994. History of precious coral fishery in Hawaii. Precious Coral & Octocoral Research, 3. 1-18.

Hare, S.R., Mantua, N.J., Francis, R.C. 1999. Inverse production regimes: Alakan and West Coast Salmon. Fisheries. 24: 6-14.

Heikoop, J.M., Hickmott, D.D., Risk, M.J., Shearer, C.K., Atudorei, V. 2002. Potential Potential climate signals from the deep-sea gorgonian coral *Primnoa Resedaeformis.* 471:117-124.

Hernandez-Leon, S., Almeida, C., Aristegui, J., Yebra, L. 2005. Lunar cycle of zooplankton biomass in subtropical waters: Biogeochemical implications. Journal of Plankton Research. 24(9). 935-939.

Howell, P. 2001. ARAND time series and spectral analysis package for the Macintosh, Brown University. IGBP PAGES/World Data Center for Paleoclimatology Data Contribution Series #2001-031. NOAA/NGDC Paleoclimatology Program, Boulder, Colorado, USA.

Karl, D.M., Christian, J.R., Dore, J.E., Hebel, D.V., Letelier, R.M., Tupas, L.M., Winn, C.D. 1996. Seasonal and interannual variability in primary production flux at station ALOHA. Deep-Sea Research II. 43(2-3): 539-568.

Karl, D.M., Lukas, R. 1996. The Hawaii Ocean Time-series (HOT) program: background, rationale and field implementation. Deep-Sea Research II. 43, no 2-3: 129-156.

Kennan, S.C., and Lukas, R. 1996. Saline intrusions in the intermediate waters north of Oahu, HI. Deep-Sea Research II. 43 no 2-3: 215-241.

Lazier, A.V., Smith, J.E., Risk, M.J., Schwarcz, H.P. 1999. The Skeletal Structure of *Desmophyllum cristagalli*: the use of deep-water corals in sclerochronology. Lethaia. 32: 119-130.

Letelier, R. M., D. M. Karl, M. R. Abbott, P. Flament, M. H. Freilich, R. Lukas, and P. T. Strub, "Role of late winter mesoscale events in the biogeochemical variability of the upper water column of the North Pacific Subtropical Gyre", J. Geophys. Res., 105, 28,723-28,739 (2000). Correction in J. Geophy. Res., 106, 7181-7182 (2000).

Levitus, S., Antonov, J.I., Boyer, T.P. 1994, Interannual Variability of temperature at a depth of 125 meters in the North Atlantic Ocean. Science, 266. 96-99.

Lewis, J.C., Barnowski, T.F., Telesnicki, G.J. 1992. Characteristics of Carbonates of Gorgonin Axes (Coelenterata, Octocorallia). Biol. Bull. 183: 278-296.

Lukas, R. 2001. Freshening of the upper thermocline in the North Pacific subtropical gyre associated with decadal changes in rainfall. Geophysical Research Letters. 28(18): 3485-3488.

Lukas, R., Santiago-Mandujano, F. 2001. Extreme water mass anomaly observed in the Hawaiian Ocean Time-series. Geophysical Research Letters. 28(15): 2931-2934.

Mangini, A., Lomitschka, M., Eichstadter, R., Frank, N., Vogler, S., Bonani, G., Hajdas, L., Patzold, J. 1998. Coral provides a way to age deep water. Nature. 392. .

Mantua, N.J., Hare, S.R., Zhang, Y., Wallace, J.M., Francis, R.C. 1997. A Pacific Interdecadal Climate Oscillation with Impacts on Salmon Production. Bulletin of the American Meteorological Society. 78: 1069-1079.

Mantua, N.J., and Hare, S.R. 2002. The Pacific Decadal Oscillation. Journal of Oceanography. 58: 35-44.

McConnaughey, T. 1988. Biomineralization Mechanisms. In the Origin, Evolution, and Modern Aspects of Biomineralization in animals and plants (ed F.C. Crick) Elsevier (1989).

McConnaughey, T. 1989a. ^{13}C and ^{18}O isotopic disequilibrium in biological carbonates: I, Patterns. Geochmica et Cosmochimica Acta. 53: 151-162.

McConnaughey, T. 1989b. ^{13}C and ^{18}O isotopic disequilibrium in biological carbonate: II. In vitro simulation of kinetic isotope effects. Geochmica et Cosmochimica Acta, 53: 163-171.

McConnaughey, T.A. 2003. Sub-equilibrium oxygen-18 and carbon-13 levels in biological carbonates: Carbonate and kinetic models. Coral Reefs. 22(4). 316-327.

Miller, A.J., White, W.B., Cayan, D.R. 1997. North Pacific Thermocline Variations on ENSO Timescales. American Meteorological Society. 2023-2039.

Miller, M.W. 1995. Growth of a temperate coral: effects of temperature, light, depth and heterotrphy. Marine Ecology Progress Series. 122:217-225.

Nitta, T., Yamada, S. 1989. Recent warming of tropical sea surface temperature and its relationship to the Northern Hemisphere circulation. Meteorological Society of Japan, Journal, 67. 375-383.

Nozaki, Y. 1997. A fresh look at element distribution in the North Pacific. Eos Trans. AGU.

Risk, M.J., Heikoop, J.M., Snow, M.G., Beukens, R. 2002. Lifespans and growth patterns of two deep-sea corals: Primnoan resedaeformis and Desmophyllum cristagalli. Hydrobiologia 471: 125-131.

Roark, B.E., Guilderson, T., Flood-Page, S.,Dunbar, R.B., Ingram, L.B. 2003. Radiocarbon Based Age Growth Rate Estimates on Deep-Sea Corals from the Pacific. 2nd International Symposium on Deep Sea Corals, Erlangen, Germany.

Roark, E.B., T.P. Guilderson, S. Flood-Page, R.B. Dunbar, B.L. Ingram, S. Fallon, and M. McCulloch, 2005, Radiocarbon-Based Ages and Growth Rates of Bamboo Corals from the Gulf of Alaska, Geophysical Research Letters, 32, doi:10.1029/2004GL021919.

Roden, G.I. 1979. On the subtropical frontal zone north of Hawaii during winter. Journal of Physical Oceanography. 10: 342-362.

Scneider, N., Miller, A.J. 2005. Predicting Western North Pacific Ocean climate. Journal of Climate. 14(20). 3997-4002.

Spero, H.J., Jang, N.A., Adkins, J.F. 2003 Geochemistry of the deep water bamboo coral (Isidella); Intermediate Depth and Surface Ocean Chemical Recorder. Eos Trans. AGU 84(46).

Stanley, G.D., Cairns, S.D. 1988. Constructional azooxanthellate coral communities; an overview with implications for the fossil records. PALAIOS. 3(2), 233-242.

Stuiver, M., Polach, H.A. 1977. Discussion: Reporting of ^{14}C data. Radiocarbon 19(3): 355-363.

Sverdrup, H., Johnson, H.W., Fleming, R.H. The Oceans: Their Physics, Chemistry and General Biology, 1087 pp., Prentiss-Hall, Old Tappan NJ. 1942.

Swart, P.K., Szmant, A., Porter, J.W., Dodge, R.E., Tougas, J.I., Shoutham, J.R. 2005. The isotopic composition of respired carbon dioxide in scleractinian coral: Implications for cycling of organic carbon in carbon.

Talley, L.D., and W.B. White, 1987. Estimates of time and space scales in the mid-latitude
North Pacific from the TRANSPAC XBT survey. J. Phys. Oceanogr., 17, 2168-2188.

Trenberth, K.E. 1990. Recent Observed Interdecadal climate changes in the northern Hemisphere. The American Meteorological Society. 71(7): 988-992.

Van Scoy, K., Olson, D.B., Fine, R.A. 1991. Ventilation of the North Pacific intermediate water: the role of the Alaskan Gyre. J. Geophys. Res. 96: 16801-16810.

Wang, B., R. Wu, and R. Lukas. 2000. Annual adjustment of thermocline in the tropical Pacific Ocean. *J. Climate*, 13, 596-616

Segment	Sample	d13C	d18O	Rep. d13C	Rep. Diff.	Rep. d18O
AT97-1	1	-4.148	-0.182			
AT97-1	2	-4.421	-0.380			
AT97-1	3	-3.741	-0.108	-3.720, -3.762	0.042	-0.105, -0.111
AT97-1	4	-3.460	-0.002			
AT97-1	5	-3.973	-0.284			
AT97-1	6	-3.720	-0.177			
AT97-1	7	-3.353	-0.115			
AT97-1	8	-3.440	-0.144	-3.385, -3.495	0.110	-0.076, -0.212
AT97-1	9	-2.929	0.109			
AT97-1	10	-2.863	0.095			
AT97-1	11	-2.251	0.480			
AT97-1	12	-2.300	0.501			
AT97-1	14	-2.319	0.408			
AT97-1	15	-2.596	0.202			
AT97-1	16	-2.576	0.318			
AT97-1	17	-2.758	0.127			
AT97-1	18	-2.615	0.245	-2.586, -2.645	0.059	0.262, 0.229
AT97-1	19	-3.247	0.095			
AT97-1	20	-3.287	0.170			
AT97-1	21	-3.554	-0.055			
AT97-1	22	-3.342	0.009			
AT97-1	23	-3.104	0.001			
AT97-1	25	-2.600	0.251			
AT97-1	26	-2.476	0.269	-2.501, -2.451	0.050	0.265, 0.272
AT97-1	27	-2.002	0.348			
AT97-1	28	-1.922	0.340			
AT97-1	29	-1.143	0.727			
AT97-1	30	-1.131	0.681			
AT97-1	31	-1.083	0.554			
AT97-1	32	-1.034	0.616			
AT97-1	33	-0.906	0.798			
AT97-1	34	-0.767	0.844			
AT97-1	35	-0.618	0.917			
AT97-1	36	-0.514	1.007			
AT97-1	37	-0.520	0.951			
AT97-1	38	-0.511	0.853			
AT97-1	39	-0.520	0.914	-0.492, -0.548	0.056	0.958, 0.870
AT97-1	40	-0.499	0.909			
AT97-1	41	-0.540	0.878			
AT97-1	42	-0.461	0.861			

AT97-1	43	-0.616	0.839			
AT97-1	45	-0.561	0.931			
AT97-1	46	-0.631	0.932			
AT97-1	47	-0.630	1.017			
AT97-1	48	-0.654	0.922			
AT97-1	49	-0.745	0.778			
AT97-1	50	-0.698	0.843			
AT97-1	51	-0.628	0.848			
AT97-1	52	-0.673	0.834			
AT97-1	53	-0.674	0.849			
AT97-1	54A	-0.660	0.849			
AT97-1	55	-0.496	0.859			
AT97-1	56	-0.528	0.914			
AT97-1	57	-0.538	1.002			
AT97-1	58	-0.545	0.915			
AT97-1	59	-0.625	0.877			
AT97-1	60	-0.608	0.963	-0.599, -0.616	0.017	1.011, 0.914
AT97-1	61	-0.551	1.108			
AT97-1	62	-0.630	0.832			
AT97-1	63	-0.488	1.060			
AT97-1	64	-0.510	1.023			
AT97-1	65	-0.581	1.013			
AT97-1	66	-0.621	0.938			
AT97-1	67	-0.587	0.953	-0.595, -0.578	0.017	0.936, 0.970
AT97-1	68	-0.699	0.855			
AT97-1	69	-0.593	0.963			
AT97-1	70	-0.664	0.934			
AT97-1	71	-0.595	0.989			
AT97-1	72	-0.644	0.954			
AT97-1	74	-0.594	0.921	-0.588, -0.599	0.011	0.943, 0.899
AT97-1	75	-0.714	0.759			
AT97-1	76	-0.600	0.976			
AT97-1	77	-0.716	0.962			
AT97-1	78	-0.593	1.046			
AT97-1	79	-0.511	1.003			
AT97-1	81	-0.665	0.968			
AT97-1	82	-0.671	0.951			
AT97-1	83	-0.723	0.931			
AT97-1	84	-0.716	0.934			
AT97-1	85	-0.854	0.803			
AT97-1	86	-0.971	0.745			
AT97-1	87	-0.900	0.840			
AT97-1	88	-1.111	0.743			

AT97-1	89	-1.043	0.556			
AT97-1	90	-1.025	0.461			
AT97-1	91	-1.204	0.614			
AT97-1	92	-1.142	0.644			
AT97-1	94	-1.035	0.726			
AT97-1	95	-1.324	0.567			
AT97-1	96	-1.486	0.556			
AT97-1	97	-1.426	0.600			
AT97-1	102	-1.550	0.490			

Segment	Rep. Diff.	Analysis Date	Running age	Cal years
AT97-1		13/7/03	0.01	1992.59
AT97-1		13/7/03	1.88	1990.72
AT97-1	0.006	13/7/03	3.76	1988.84
AT97-1		13/7/03	5.63	1986.97
AT97-1		13/7/03	7.51	1985.09
AT97-1		13/7/03	9.38	1983.22
AT97-1		13/7/03	11.25	1981.35
AT97-1	0.136	13/7/03	13.13	1979.47
AT97-1		13/7/03	15.00	1977.60
AT97-1		13/7/03	16.88	1975.72
AT97-1		13/7/03	18.75	1973.85
AT97-1		13/7/03	22.58	1970.03
AT97-1		13/7/03	30.23	1962.38
AT97-1		13/7/03	34.05	1958.55
AT97-1		13/7/03	37.88	1954.73
AT97-1		13/7/03	41.70	1950.90
AT97-1	0.033	13/7/03	45.53	1947.08
AT97-1		13/7/03	49.35	1943.25
AT97-1		13/7/03	53.18	1939.43
AT97-1		13/7/03	57.00	1935.60
AT97-1		13/7/03	59.80	1932.80
AT97-1		13/7/03	62.60	1930.00
AT97-1		13/7/03	68.20	1924.40
AT97-1	0.007	13/7/03	71.00	1921.60
AT97-1		13/7/03	73.80	1918.80
AT97-1		13/7/03	76.60	1916.00
AT97-1		13/7/03	79.40	1913.20
AT97-1		13/7/03	82.20	1910.40
AT97-1		13/7/03	85.00	1907.60
AT97-1		13/7/03	87.80	1904.80
AT97-1		14/7/03	90.60	1902.00
AT97-1		14/7/03	93.40	1899.20
AT97-1		14/7/03	96.20	1896.40
AT97-1		14/7/03	99.00	1893.60
AT97-1		14/7/03	101.59	1891.01
AT97-1		14/7/03	104.18	1888.42
AT97-1	0.088	14/7/03	106.77	1885.83
AT97-1		14/7/03	109.36	1883.24
AT97-1		14/7/03	111.95	1880.65
AT97-1		14/7/03	114.55	1878.05

AT97-1		14/7/03	117.14	1875.46
AT97-1		14/7/03	122.32	1870.28
AT97-1		14/7/03	124.91	1867.69
AT97-1		14/7/03	127.50	1865.10
AT97-1		14/7/03	130.09	1862.51
AT97-1		14/7/03	132.68	1859.92
AT97-1		14/7/03	135.27	1857.33
AT97-1		14/7/03	137.86	1854.74
AT97-1		14/7/03	140.45	1852.15
AT97-1		14/7/03	143.05	1849.55
AT97-1		14/7/03	145.64	1846.96
AT97-1		14/7/03	148.23	1844.37
AT97-1		14/7/03	150.82	1841.78
AT97-1		14/7/03	153.41	1839.19
AT97-1		14/7/03	156.00	1836.60
AT97-1		14/7/03	158.59	1834.01
AT97-1	0.097	14/7/03	161.18	1831.42
AT97-1		14/7/03	163.77	1828.83
AT97-1		14/7/03	166.36	1826.24
AT97-1		14/7/03	168.95	1823.65
AT97-1		14/7/03	171.55	1821.05
AT97-1		14/7/03	174.14	1818.46
AT97-1		14/7/03	176.73	1815.87
AT97-1	0.034	15/7/03	179.32	1813.28
AT97-1		15/7/03	181.91	1810.69
AT97-1		15/7/03	184.50	1808.10
AT97-1		15/7/03	187.09	1805.51
AT97-1		15/7/03	189.68	1802.92
AT97-1		15/7/03	192.27	1800.33
AT97-1	0.044	15/7/03	197.45	1795.15
AT97-1		15/7/03	200.05	1792.55
AT97-1		15/7/03	202.64	1789.96
AT97-1		15/7/03	205.23	1787.37
AT97-1		15/7/03	207.82	1784.78
AT97-1		15/7/03	210.41	1782.19
AT97-1		15/7/03	215.59	1777.01
AT97-1		15/7/03	218.18	1774.42
AT97-1		15/7/03	220.77	1771.83
AT97-1		15/7/03	223.36	1769.24
AT97-1		15/7/03	225.95	1766.65
AT97-1		15/7/03	228.55	1764.05
AT97-1		15/7/03	231.14	1761.46
AT97-1		15/7/03	233.73	1758.87

AT97-1		15/7/03	236.32	1756.28
AT97-1		15/7/03	238.91	1753.69
AT97-1		15/7/03	241.50	1751.10
AT97-1		15/7/03	244.09	1748.51
AT97-1		15/7/03	249.27	1743.33
AT97-1		15/7/03	251.86	1740.74
AT97-1		15/7/03	254.45	1738.15
AT97-1		15/7/03	257.05	1735.55
AT97-1		15/7/03	270.00	1722.60

Segment	Sample	d13C	d18O	Rep. d13C	Rep. Diff.	Rep. d18O
AM97-1	1	-3.872	-0.187	-3.918, -3.826	0.092	-0.219, -0.155
AM97-1	2	-3.879	-0.255			
AM97-1	3	-3.947	-0.369			
AM97-1	4	-4.221	-0.221			
AM97-1	5					
AM97-1	6	-4.088	-0.141			
AM97-1	7	-3.906	-0.073			
AM97-1	8	-3.237	0.185			
AM97-1	9	-3.074	0.125			
AM97-1	10					
AM97-1	11					
AM97-1	12	-1.575	0.555			
AM97-1	13	-0.973	0.747			
AM97-1	14	-0.857	0.721			
AM97-1	15	-1.004	0.654			
AM97-1	16	-0.744	0.768			
AM97-1	17	-1.044	0.637			
AM97-1	18	-1.533	0.560			
AM97-1	19	-1.449	0.538			
AM97-1	20	-1.461	0.400			
AM97-1	21	-2.163	0.152			
AM97-1	22	-1.988	0.291			
AM97-1	23	-2.033	0.180			
AM97-1	24	-2.460	-0.077			
AM97-1	25	-2.948	-0.011			
AM97-1	26	-1.983	0.528			
AM97-1	27	-2.548	0.403			
AM97-1	28	-3.177	0.158			
AM97-1	29	-3.522	-0.006			
AM97-1	30	-3.734	-0.056			
AM97-1	31	-3.872	-0.200			
AM97-1	32	-3.455	0.036			
AM97-1	33	-3.339	-0.113			
AM97-1	34	-3.338	-0.035			
AM97-1	35	-3.638	-0.307			
AM97-1	36	-3.454	-0.357			
AM97-1	37	-2.935	-0.173			

AM97-1	38	-2.211	0.188			
AM97-1	39	-1.919	0.250			
AM97-1	40	-1.784	0.614			
AM97-1	42					
AM97-1	43	-0.769	0.815			
AM97-1	44	-0.802	0.778			
AM97-1	45	-0.799	0.725			
AM97-1	46	-0.919	0.745			
AM97-1	47	-1.123	0.693			
AM97-1	48	-1.047	0.859			
AM97-1	49	-0.802	0.885			
AM97-1	50	-0.772	0.892			
AM97-1	51	-0.733	1.001			
AM97-1	52	-0.851	0.862			
AM97-1	53	-0.823	0.878			
AM97-1	54	-0.763	0.966			
AM97-1	55	-0.906	0.845			
AM97-1	56	-1.042	0.829			
AM97-1	57	-1.337	0.679			
AM97-1	58	-1.285	0.661			
AM97-1	59	-0.856	0.805			
AM97-1	60	-0.998	0.751			
AM97-1	61	-1.163	0.805			
AM97-1	62	-1.135	0.742			
AM97-1	63	-1.055	0.877			
AM97-1	64	-0.975	0.770			
AM97-1	65	-1.017	0.590			
AM97-1	66	-0.883	0.835			
AM97-1	67	-0.809	0.695	-0.838, -0.780	0.058	0.680, 0.710
AM97-1	68	-0.928	0.728			
AM97-1	69	-0.997	0.668			
AM97-1	70	-0.846	0.676			
AM97-1	71	-0.828	0.701			
AM97-1	72	-0.884	0.869			
AM97-1	73	-0.750	0.889			
AM97-1	74	-0.893	0.776	-0.811, -0.974	0.163	0.859, 0.692
AM97-1	75	-1.073	0.568			
AM97-1	76	-1.237	0.793			
AM97-1	77	-1.297	0.699			
AM97-1	78	-1.274	0.816			
AM97-1	79	-1.532	0.548			
AM97-1	80	-1.328	0.666			

AM97-1	81	-1.338	0.680			
AM97-1	82	-1.301	0.624			
AM97-1	83	-1.248	0.565			
AM97-1	84	-1.256	0.534			
AM97-1	85	-1.035	0.614			
AM97-1	86	-0.923	0.623			
AM97-1	87	-1.102	0.492			
AM97-1	88	-0.905	0.535			
AM97-1	89	-0.735	0.504			
AM97-1	90	-0.773	0.432			
AM97-1	91	-0.934	0.522			
AM97-1	92	-1.503	0.276			
AM97-1	93	-0.796	0.634			
AM97-1	94	-1.131	0.495			
AM97-1	95	-1.248	0.508			
AM97-1	96	-0.728	0.573			
AM97-1	97	-0.839	0.333			
AM97-1	98	-0.701	0.497			
AM97-1	99	-0.842	0.469			
AM97-1	100	-0.658	0.545			
AM97-1	101	-0.743	0.551			

Segment	Rep. Diff.	Analysis Date	Comments	Running age	Cal years
AM97-1	0.064	10/7/03		0.01	1992.59
AM97-1		10/7/03		1.26	1991.34
AM97-1		10/7/03		2.51	1990.09
AM97-1		10/7/03		3.76	1988.84
AM97-1		10/7/03	Insufficient sample for good analysis		
AM97-1		10/7/03		6.26	1986.34
AM97-1		10/7/03		7.51	1985.09
AM97-1		10/7/03		8.76	1983.84
AM97-1		10/7/03		10.01	1982.59
AM97-1		10/7/03	Insufficient sample for good analysis		
AM97-1		10/7/03	Insufficient sample for good analysis		
AM97-1		10/7/03		13.76	1978.84
AM97-1		10/7/03		15.01	1977.60
AM97-1		10/7/03		16.25	1976.35
AM97-1		10/7/03		17.50	1975.10
AM97-1		10/7/03		18.75	1973.85
AM97-1		10/7/03		20.00	1972.60
AM97-1		10/7/03		21.25	1971.35
AM97-1		10/7/03		22.50	1970.10
AM97-1		10/7/03		23.75	1968.85
AM97-1		10/7/03		25.00	1967.60
AM97-1		10/7/03		26.25	1966.35
AM97-1		10/7/03		27.50	1965.10
AM97-1		10/7/03		28.75	1963.85
AM97-1		10/7/03		30.00	1962.60
AM97-1		10/7/03		32.47	1960.13
AM97-1		10/7/03		34.93	1957.67
AM97-1		10/7/03		37.40	1955.20
AM97-1		10/7/03		39.87	1952.73
AM97-1		10/7/03		42.33	1950.27
AM97-1		10/7/03		44.80	1947.80
AM97-1		10/7/03		47.27	1945.33
AM97-1		10/7/03		49.73	1942.87
AM97-1		11/7/03		52.20	1940.40
AM97-1		11/7/03		54.67	1937.93
AM97-1		11/7/03		57.13	1935.47
AM97-1		11/7/03		59.60	1933.00

AM97-1		11/7/03		62.07	1930.53
AM97-1		11/7/03		64.53	1928.07
AM97-1		11/7/03		67.00	1925.60
AM97-1		11/7/03	Insufficient sample for good analysis		
AM97-1		11/7/03		75.33	1917.27
AM97-1		11/7/03		78.11	1914.49
AM97-1		11/7/03		80.89	1911.71
AM97-1		11/7/03		83.67	1908.93
AM97-1		11/7/03		86.44	1906.16
AM97-1		11/7/03		89.22	1903.38
AM97-1		11/7/03		92.00	1900.60
AM97-1		11/7/03		95.57	1897.03
AM97-1		11/7/03		99.14	1893.46
AM97-1		11/7/03		102.71	1889.89
AM97-1		11/7/03		106.29	1886.31
AM97-1		11/7/03		109.86	1882.74
AM97-1		11/7/03		113.43	1879.17
AM97-1		11/7/03		117.00	1875.60
AM97-1		11/7/03		120.57	1872.03
AM97-1		11/7/03		124.14	1868.46
AM97-1		11/7/03		127.71	1864.89
AM97-1		11/7/03		131.29	1861.31
AM97-1		11/7/03		134.86	1857.74
AM97-1		11/7/03		138.43	1854.17
AM97-1		11/7/03		142.00	1850.60
AM97-1		11/7/03		145.85	1846.75
AM97-1		11/7/03		149.69	1842.91
AM97-1		11/7/03		153.54	1839.06
AM97-1	0.030	11/7/03		157.38	1835.22
AM97-1		12/7/03		161.23	1831.37
AM97-1		12/7/03		165.08	1827.52
AM97-1		12/7/03		168.92	1823.68
AM97-1		12/7/03		172.77	1819.83
AM97-1		12/7/03		176.62	1815.98
AM97-1		12/7/03		180.46	1812.14
AM97-1	0.167	12/7/03		184.31	1808.29
AM97-1		12/7/03		188.15	1804.45
AM97-1		12/7/03		192.00	1800.60
AM97-1		12/7/03		195.85	1796.75
AM97-1		12/7/03		199.69	1792.91
AM97-1		12/7/03		203.54	1789.06
AM97-1		12/7/03		207.38	1785.22

AM97-1		12/7/03		211.23	1781.37
AM97-1		12/7/03		215.08	1777.52
AM97-1		12/7/03		218.92	1773.68
AM97-1		12/7/03		222.77	1769.83
AM97-1		12/7/03		226.62	1765.98
AM97-1		12/7/03		230.46	1762.14
AM97-1		12/7/03		234.31	1758.29
AM97-1		12/7/03		238.15	1754.45
AM97-1		12/7/03		242.00	1750.60
AM97-1		12/7/03		244.55	1748.05
AM97-1		12/7/03		247.09	1745.51
AM97-1		12/7/03		249.64	1742.96
AM97-1		12/7/03		252.18	1740.42
AM97-1		12/7/03		254.73	1737.87
AM97-1		12/7/03		257.27	1735.33
AM97-1		12/7/03		259.82	1732.78
AM97-1		12/7/03		262.36	1730.24
AM97-1		12/7/03		264.91	1727.69
AM97-1		12/7/03		267.45	1725.15
AM97-1		12/7/03		270.00	1722.60
AM97-1		12/7/03		272.55	1720.05

Segment	Sample	d13C	d18O	Rep. d13C	Rep. Diff.	Rep. d18O
AB97-1	1	-1.059	0.279			
AB97-1	2	-0.852	0.253			
AB97-1	3	-0.994	0.154	-0.966, -1.021	0.055	0.169, 0.139
AB97-1	4	-1.093	0.168			
AB97-1	5	-0.883	0.458			
AB97-1	6	-0.921	0.423			
AB97-1	7	-0.831	0.345			
AB97-1	8	-0.898	0.318			
AB97-1	9	-0.971	0.299			
AB97-1	10	-0.951	0.244			
AB97-1	11	-0.858	0.338	-0.876, -0.840	0.036	0.354, 0.321
AB97-1	12	-0.911	0.418			
AB97-1	13	-0.960	0.317			
AB97-1	14	-0.848	0.358			
AB97-1	15	-0.837	0.306			
AB97-1	16	-0.838	0.308			
AB97-1	17	-0.932	0.341			
AB97-1	17.5	-0.946	0.232			
AB97-1	18	-0.871	0.334			
AB97-1	19	-0.884	0.294	-0.840, -0.927	0.087	0.301, 0.286
AB97-1	20	-0.946	0.304			
AB97-1	21	-0.747	0.437			
AB97-1	22	-0.896	0.298			
AB97-1	23	-0.750	0.380			
AB97-1	24	-0.753	0.353			
AB97-1	25	-0.755	0.342			
AB97-1	26.5	-0.662	0.524			
AB97-1	28	-0.884	0.333	-0.871, -0.897	0.026	0.333, 0.332
AB97-1	29	-0.839	0.442			
AB97-1	30	-0.789	0.280			
AB97-1	31	-0.814	0.531			
AB97-1	32	-0.839	0.544			
AB97-1	33	-0.866	0.484	-0.886, -0.846	0.040	0.512, 0.456
AB97-1	34	-0.780	0.583			
AB97-1	35	-0.862	0.504			
AB97-1	36	-0.891	0.518			
AB97-1	37	-0.843	0.727			
AB97-1	38	-0.818	0.704			
AB97-1	39	-0.663	0.806			
AB97-1	40	-0.748	0.723	-0.780, -0.716	0.064	0.695, 0.750
AB97-1	41	-0.710	0.665			

AB97-1	42	-0.655	0.679			
AB97-1	43	-0.618	0.725			
AB97-1	44	-0.578	0.766			
AB97-1	45	-0.626	0.695			
AB97-1	46	-0.542	0.780			
AB97-1	47	-0.682	0.752			
AB97-1	48	-0.751	0.763			
AB97-1	49	-0.785	0.737	-0.774, -0.796	0.022	0.745, 0.728
AB97-1	50	-0.624	0.663			
AB97-1	51	-0.696	0.632			
AB97-1	52	-0.834	0.623			
AB97-1	53	-1.085	0.587			
AB97-1	54	-0.987	0.604			
AB97-1	55	-0.964	0.469			
AB97-1	56	-1.254	0.272			
AB97-1	57	-1.203	0.462	-1.210, -1.196	0.014	0.502, 0.422
AB97-1	58	-1.365	0.473			
AB97-1	59	-1.407	0.331			
AB97-1	60	-1.113	0.419			
AB97-1	61	-0.921	0.654			
AB97-1	62.5	-0.600	0.783			
AB97-1	64	-0.484	0.787			
AB97-1	65	-0.586	0.737			
AB97-1	66	-0.662	0.754			
AB97-1	67	-0.736	0.721			
AB97-1	68	-0.649	0.681			
AB97-1	69	-0.813	0.596			
AB97-1	70	-0.877	0.527			
AB97-1	71	-0.687	0.553	-0.705, -0.669	0.036	0.565, 0.541
AB97-1	72	-0.615	0.642			
AB97-1	73	-0.638	0.558			
AB97-1	74	-0.583	0.543			
AB97-1	75	-0.616	0.558			
AB97-1	76	-0.497	0.563			
AB97-1	77	-0.524	0.524			
AB97-1	78	-0.389	0.647	-0.402, -0.375	0.027	0.602, 0.691
AB97-1	79	-0.512	0.633			
AB97-1	80	-0.479	0.771			
AB97-1	81	-0.557	0.693			
AB97-1	82	-0.581	0.757			
AB97-1	83	-0.791	0.584			
AB97-1	84	-0.844	0.619			
AB97-1	85	-0.674	0.682			

AB97-1	86	-0.638	0.711			
AB97-1	87	-0.662	0.521			
AB97-1	88	-0.664	0.544			
AB97-1	89	-0.740	0.445			
AB97-1	90	-0.485	0.637			
AB97-1	91	-0.298	0.648			
AB97-1	92	-0.340	0.652			
AB97-1	96	-0.863	0.416			
AB97-1	97	-0.423	0.560			

Segment	Rep. Diff.	Analysis Date	Running Age	Cal.Years
AB97-1		7/7/2003	0.01	1992.59
AB97-1		7/7/2003	0.43	1992.17
AB97-1	0.030	7/7/2003	0.84	1991.76
AB97-1		7/7/2003	1.26	1991.34
AB97-1		7/7/2003	1.68	1990.92
AB97-1		7/7/2003	2.09	1990.51
AB97-1		7/7/2003	2.51	1990.09
AB97-1		7/7/2003	2.93	1989.67
AB97-1		7/7/2003	3.34	1989.26
AB97-1		7/7/2003	3.76	1988.84
AB97-1	0.033	7/7/2003	4.17	1988.43
AB97-1		7/7/2003	4.59	1988.01
AB97-1		7/7/2003	5.01	1987.59
AB97-1		7/7/2003	5.42	1987.18
AB97-1		7/7/2003	5.84	1986.76
AB97-1		7/7/2003	6.26	1986.34
AB97-1		7/7/2003	6.67	1985.93
AB97-1		7/7/2003	6.88	1985.72
AB97-1		7/7/2003	7.09	1985.51
AB97-1	0.015	7/7/2003	7.51	1985.09
AB97-1		7/7/2003	7.92	1984.68
AB97-1		7/7/2003	8.34	1984.26
AB97-1		7/7/2003	8.76	1983.84
AB97-1		7/7/2003	9.17	1983.43
AB97-1		7/7/2003	9.59	1983.01
AB97-1		7/7/2003	10.00	1982.60
AB97-1		7/7/2003	10.63	1981.97
AB97-1	0.001	7/7/2003	11.25	1981.35
AB97-1		7/7/2003	11.67	1980.93
AB97-1		7/7/2003	12.09	1980.51
AB97-1		7/8/2003	12.50	1980.10
AB97-1		7/8/2003	12.92	1979.68
AB97-1	0.056	7/8/2003	13.34	1979.26
AB97-1		7/8/2003	13.75	1978.85
AB97-1		7/8/2003	14.17	1978.43
AB97-1		7/8/2003	14.59	1978.01
AB97-1		7/8/2003	15.00	1977.60
AB97-1		7/8/2003	15.42	1977.18
AB97-1		7/8/2003	15.83	1976.77
AB97-1	0.055	7/8/2003	16.25	1976.35
AB97-1		7/8/2003	16.67	1975.93

AB97-1		7/8/2003	17.08	1975.52
AB97-1		7/8/2003	17.50	1975.10
AB97-1		7/8/2003	17.92	1974.68
AB97-1		7/8/2003	18.33	1974.27
AB97-1		7/8/2003	18.75	1973.85
AB97-1		7/8/2003	21.69	1970.91
AB97-1		7/8/2003	24.63	1967.97
AB97-1	0.017	7/8/2003	27.58	1965.02
AB97-1		7/8/2003	30.52	1962.08
AB97-1		7/8/2003	33.46	1959.14
AB97-1		7/8/2003	36.40	1956.20
AB97-1		7/8/2003	39.35	1953.25
AB97-1		7/8/2003	42.29	1950.31
AB97-1		7/8/2003	45.23	1947.37
AB97-1		7/8/2003	48.17	1944.43
AB97-1	0.080	7/8/2003	51.12	1941.48
AB97-1		7/8/2003	54.06	1938.54
AB97-1		7/8/2003	57.00	1935.60
AB97-1		7/8/2003	65.40	1927.20
AB97-1		7/9/2003	73.80	1918.80
AB97-1		7/9/2003	86.40	1906.20
AB97-1		7/9/2003	99.00	1893.60
AB97-1		7/9/2003	104.18	1888.42
AB97-1		7/9/2003	109.36	1883.24
AB97-1		7/9/2003	114.55	1878.05
AB97-1		7/9/2003	119.73	1872.87
AB97-1		7/9/2003	124.91	1867.69
AB97-1		7/9/2003	130.09	1862.51
AB97-1	0.024	7/9/2003	135.27	1857.33
AB97-1		7/9/2003	140.45	1852.15
AB97-1		7/9/2003	145.64	1846.96
AB97-1		7/9/2003	150.82	1841.78
AB97-1		7/9/2003	156.00	1836.60
AB97-1		7/9/2003	161.18	1831.42
AB97-1		7/9/2003	166.36	1826.24
AB97-1	0.089	7/9/2003	171.55	1821.05
AB97-1		7/9/2003	176.73	1815.87
AB97-1		7/9/2003	181.91	1810.69
AB97-1		7/9/2003	187.09	1805.51
AB97-1		7/9/2003	192.27	1800.33
AB97-1		7/9/2003	197.45	1795.15
AB97-1		7/9/2003	202.64	1789.96
AB97-1		7/9/2003	207.82	1784.78

AB97-1		7/9/2003	213.00	1779.60
AB97-1		7/9/2003	218.18	1774.42
AB97-1		7/9/2003	223.36	1769.24
AB97-1		7/9/2003	228.55	1764.05
AB97-1		7/9/2003	233.73	1758.87
AB97-1		7/9/2003	238.91	1753.69
AB97-1		7/9/2003	244.09	1748.51
AB97-1		7/9/2003	264.82	1727.78
AB97-1		7/9/2003	270.00	1722.60

Segment	Sample	d13C	d18O	Rep. d13C	Rep. Diff.	Rep. d18O
AT97-2	1	-1.060	0.671			
AT97-2	2	-1.001	0.617			
AT97-2	3	-1.017	0.652			
AT97-2	4	-0.969	0.698			
AT97-2	5	-0.984	0.693			
AT97-2	6	-0.934	0.548	-0.940, -0.928	0.012	0.566, 0.529
AT97-2	7	-0.912	0.621			
AT97-2	8	-0.920	0.579			
AT97-2	9	-0.876	0.696			
AT97-2	10	-0.881	0.749			
AT97-2	11	-0.989	0.635			
AT97-2	12	-0.925	0.558			
AT97-2	13	-0.962	0.480			
AT97-2	14	-0.933	0.541			
AT97-2	15	-0.899	0.658			
AT97-2	16	-0.987	0.619			
AT97-2	17	-0.961	0.647			
AT97-2	18	-0.999	0.602	-1.006, -0.991	0.015	0.594, 0.610
AT97-2	19	-0.945	0.591			
AT97-2	20	-0.945	0.588			
AT97-2	21	-0.952	0.488			
AT97-2	22	-0.871	0.755			
AT97-2	23	-1.100	0.627			
AT97-2	24	-1.131	0.699			
AT97-2	25	-1.012	0.695			
AT97-2	27	-1.170	0.553	-1.259, -1.080	0.179	0.535, 0.571
AT97-2	28	-1.272	0.586			
AT97-2	29	-1.079	0.686			
AT97-2	30	-1.182	0.652			
AT97-2	31	-1.267	0.570			
AT97-2	32	-1.214	0.653			
AT97-2	33	-0.968	0.825			
AT97-2	34	-0.832	0.838			
AT97-2	35	-0.718	0.741			
AT97-2	36	-0.702	0.758			
AT97-2	37	-0.795	0.759			
AT97-2	38	-0.888	0.780			
AT97-2	39	-0.951	0.796			
AT97-2	40	-1.120	0.797			
AT97-2	41	-1.350	0.656			
AT97-2	42	-1.536	0.767			
AT97-2	43	-1.284	0.696			

AT97-2	44	-1.333	0.682			
AT97-2	45	-1.458	0.609			
AT97-2	46	-1.192	0.687	-1.174, -1.209	0.035	0.724, 0.650
AT97-2	47	-0.983	0.844			
AT97-2	48	-1.008	0.880			
AT97-2	49	-1.093	0.764			
AT97-2	51	-0.737	0.870			
AT97-2	52	-0.579	0.904			
AT97-2	53	-0.702	0.747			
AT97-2	54	-0.689	0.868			
AT97-2	55	-0.873	0.775			
AT97-2	56	-0.726	0.877			
AT97-2	57	-0.662	0.887			
AT97-2	58	-0.571	0.810			
AT97-2	59	-0.516	0.680			
AT97-2	60	-0.498	0.841			
AT97-2	61	-0.403	0.792			
AT97-2	62	-0.395	0.746			
AT97-2	63	-0.429	0.753			
AT97-2	64	-0.531	0.804			
AT97-2	65	-0.387	0.782			
AT97-2	67	-0.423	0.805			
AT97-2	68	-0.463	0.831			
AT97-2	69	-0.491	0.805			
AT97-2	70	-0.540	0.768			
AT97-2	71	-0.398	0.772			
AT97-2	72	-0.334	0.839			
AT97-2	73	-0.236	0.832			

Rep. Diff.	Segment	Analysis Date	Running age	Cal years
	AT97-2	29/7/03	0.01	1997.59
	AT97-2	29/7/03	0.36	1997.24
	AT97-2	29/7/03	0.70	1996.90
	AT97-2	29/7/03	1.05	1996.55
	AT97-2	29/7/03	1.40	1996.20
0.037	AT97-2	29/7/03	1.75	1995.85
	AT97-2	29/7/03	2.09	1995.51
	AT97-2	29/7/03	2.44	1995.16
	AT97-2	29/7/03	2.79	1994.81
	AT97-2	29/7/03	3.13	1994.47
	AT97-2	29/7/03	3.48	1994.12
	AT97-2	29/7/03	3.83	1993.77
	AT97-2	29/7/03	4.18	1993.43
	AT97-2	29/7/03	4.52	1993.08
	AT97-2	29/7/03	4.87	1992.73
	AT97-2	29/7/03	5.22	1992.38
	AT97-2	29/7/03	5.56	1992.04
0.016	AT97-2	29/7/03	5.91	1991.69
	AT97-2	29/7/03	6.26	1991.34
	AT97-2	29/7/03	6.60	1991.00
	AT97-2	29/7/03	6.95	1990.65
	AT97-2	29/7/03	7.30	1990.30
	AT97-2	29/7/03	7.65	1989.95
	AT97-2	29/7/03	7.99	1989.61
	AT97-2	29/7/03	8.34	1989.26
0.036	AT97-2	29/7/03	9.03	1988.57
	AT97-2	29/7/03	9.38	1988.22
	AT97-2	29/7/03	9.73	1987.87
	AT97-2	29/7/03	10.08	1987.52
	AT97-2	29/7/03	10.42	1987.18
	AT97-2	29/7/03	10.77	1986.83
	AT97-2	29/7/03	11.12	1986.48
	AT97-2	29/7/03	11.46	1986.14
	AT97-2	29/7/03	11.81	1985.79
	AT97-2	29/7/03	12.16	1985.44
	AT97-2	29/7/03	12.51	1985.10
	AT97-2	29/7/03	12.85	1984.75
	AT97-2	29/7/03	13.20	1984.40
	AT97-2	29/7/03	13.55	1984.05
	AT97-2	29/7/03	13.89	1983.71
	AT97-2	29/7/03	14.24	1983.36
	AT97-2	29/7/03	14.59	1983.01

	AT97-2	29/7/03	14.93	1982.67
	AT97-2	29/7/03	15.28	1982.32
0.074	AT97-2	29/7/03	15.63	1981.97
	AT97-2	30/7/03	15.98	1981.62
	AT97-2	30/7/03	16.32	1981.28
	AT97-2	30/7/03	16.67	1980.93
	AT97-2	30/7/03	17.36	1980.24
	AT97-2	30/7/03	17.71	1979.89
	AT97-2	30/7/03	18.06	1979.54
	AT97-2	30/7/03	18.41	1979.19
	AT97-2	30/7/03	18.75	1978.85
	AT97-2	30/7/03	19.10	1978.50
	AT97-2	30/7/03	19.45	1978.15
	AT97-2	30/7/03	19.79	1977.81
	AT97-2	30/7/03	20.14	1977.46
	AT97-2	30/7/03	20.49	1977.11
	AT97-2	30/7/03	20.84	1976.77
	AT97-2	30/7/03	21.18	1976.42
	AT97-2	30/7/03	21.53	1976.07
	AT97-2	30/7/03	21.88	1975.72
	AT97-2	30/7/03	22.22	1975.38
	AT97-2	30/7/03	22.92	1974.68
	AT97-2	30/7/03	23.26	1974.34
	AT97-2	30/7/03	23.61	1973.99
	AT97-2	30/7/03	23.96	1973.64
	AT97-2	30/7/03	24.31	1973.29
	AT97-2	30/7/03	24.65	1972.95
	AT97-2	30/7/03	25.00	1972.60

Segment	Sample	d13C	d18O	Rep. d13C	Rep. Diff.	Rep. d18O
AB97-2	1	-0.732	0.761			
AB97-2	2	-0.745	0.709	-0.709, -0.781	0.072	0.753, 0.665
AB97-2	3	-0.701	0.593			
AB97-2	4	-0.766	0.746			
AB97-2	5	-0.812	0.488			
AB97-2	6					
AB97-2	7	-0.722	0.548			
AB97-2	8	-0.644	0.755			
AB97-2	9	-0.655	0.857			
AB97-2	10	-0.618	0.868			
AB97-2	11	-0.632	0.825			
AB97-2	12	-0.710	0.746	-0.726, -0.693	0.033	0.763, 0.728
AB97-2	13	-0.729	0.768			
AB97-2	14	-0.817	0.740			
AB97-2	15	-0.846	0.638			
AB97-2	16	-0.777	0.559			
AB97-2	17	-0.720	0.467			
AB97-2	18	-0.692	0.499			
AB97-2	19	-0.730	0.372	-0.702, -0.762	0.060	0.410, 0.334
AB97-2	20	-0.717	0.360			
AB97-2	21	-0.655	0.573			
AB97-2	22	-0.654	0.710			
AB97-2	23	-0.654	0.633			
AB97-2	24	-0.680	0.545			
AB97-2	25	-0.812	0.551			
AB97-2	26	-0.809	0.531			
AB97-2	27	-0.884	0.587			
AB97-2	28	-0.933	0.525			
AB97-2	29	-0.817	0.638			
AB97-2	30	-0.878	0.544			
AB97-2	31	-0.834	0.605			
AB97-2	32	-0.911	0.694			
AB97-2	33	-0.936	0.605			
AB97-2	34	-1.051	0.674			
AB97-2	35	-1.121	0.609			
AB97-2	36	-1.124	0.629			
AB97-2	37	-1.087	0.780			
AB97-2	38	-1.034	0.569	-1.030, -1.038	0.007	0.567, 0.571
AB97-2	39	-0.805	0.693			
AB97-2	40	-0.813	0.656			

AB97-2	41	-1.052	0.699			
AB97-2	42	-1.012	0.663			
AB97-2	43	-0.999	0.571			
AB97-2	44	-0.881	0.756			
AB97-2	45	-1.031	0.706			
AB97-2	46	-1.257	0.547	-1.252, -1.262	0.010	0.531, 0.563
AB97-2	47	-1.173	0.708			
AB97-2	48	-1.023	0.775			
AB97-2	49	-0.942	0.766			
AB97-2	50	-0.854	0.774			
AB97-2	51	-0.749	0.844			
AB97-2	52	-0.602	0.832			
AB97-2	53	-0.595	0.885			
AB97-2	54	-0.992	0.859			
AB97-2	55	-1.040	0.785			
AB97-2	56	-0.908	0.739			
AB97-2	57	-0.976	0.846			
AB97-2	58	-0.862	0.777			
AB97-2	59	-1.081	0.714			
AB97-2	60	-0.945	0.871			
AB97-2	61	-0.931	0.840			
AB97-2	62	-1.007	0.766			
AB97-2	63	-1.046	0.793			
AB97-2	64	-0.894	0.834			
AB97-2	65	-1.106	0.713			
AB97-2	66	-1.133	0.713			
AB97-2	67	-0.902	0.844			
AB97-2	68	-0.760	0.862	-0.768, -0.752	0.016	0.832, 0.892
AB97-2	69	-0.605	0.813			
AB97-2	70	-0.537	0.904			
AB97-2	71	-0.702	0.860			
AB97-2	72	-1.029	0.592			
AB97-2	73	-0.886	0.653			
AB97-2	74	-0.775	0.781			
AB97-2	75	-0.630	0.820			
AB97-2	76	-0.810	0.698			
AB97-2	77	-0.828	0.722			
AB97-2	79	-0.490	0.802			
AB97-2	80	-0.484	0.792			
AB97-2	83	-0.480	0.809			
AB97-2	84	-0.378	0.884			
AB97-2	85	-0.441	0.874			
AB97-2	86	-0.552	0.896			

AB97-2	87	-0.719	0.760			
AB97-2	88	-0.804	0.650			
AB97-2	89	-0.439	0.645			
AB97-2	90	-0.487	0.623			
AB97-2	91	-0.444	0.589			
AB97-2	92	-0.881	0.358			
AB97-2	93	-0.374	0.482			

Segment	Rep. Diff.	Analysis Date	Comments	Running age	Cal years
AB97-2		16/7/03		0.01	1997.59
AB97-2	0.088	16/7/03		0.36	1997.24
AB97-2		16/7/03		0.70	1996.90
AB97-2		16/7/03		1.05	1996.55
AB97-2		16/7/03		1.40	1996.20
AB97-2		16/7/03	Insufficient sample for good analysis		
AB97-2		16/7/03		1.75	1995.85
AB97-2		16/7/03		2.44	1995.16
AB97-2		16/7/03		2.79	1994.81
AB97-2		16/7/03		3.13	1994.47
AB97-2		16/7/03		3.48	1994.12
AB97-2	0.035	16/7/03		3.83	1993.77
AB97-2		16/7/03		4.18	1993.43
AB97-2		16/7/03		4.52	1993.08
AB97-2		16/7/03		4.87	1992.73
AB97-2		16/7/03		5.22	1992.38
AB97-2		16/7/03		5.56	1992.04
AB97-2		16/7/03		5.91	1991.69
AB97-2	0.076	16/7/03		6.26	1991.34
AB97-2		16/7/03		6.60	1991.00
AB97-2		16/7/03		6.95	1990.65
AB97-2		16/7/03		7.30	1990.30
AB97-2		16/7/03		7.65	1989.95
AB97-2		16/7/03		7.99	1989.61
AB97-2		16/7/03		8.34	1989.26
AB97-2		16/7/03		8.69	1988.91
AB97-2		16/7/03		9.03	1988.57
AB97-2		16/7/03		9.38	1988.22
AB97-2		16/7/03		9.73	1987.87
AB97-2		16/7/03		10.08	1987.52
AB97-2		16/7/03		10.42	1987.18
AB97-2		17/7/03		10.77	1986.83
AB97-2		17/7/03		11.12	1986.48
AB97-2		17/7/03		11.46	1986.14
AB97-2		17/7/03		11.81	1985.79
AB97-2		17/7/03		12.16	1985.44
AB97-2		17/7/03		12.51	1985.10
AB97-2	0.004	17/7/03		12.85	1984.75
AB97-2		17/7/03		13.20	1984.40
AB97-2		17/7/03		13.55	1984.05

AB97-2		17/7/03		13.89	1983.71
AB97-2		17/7/03		14.24	1983.36
AB97-2		17/7/03		14.59	1983.01
AB97-2		17/7/03		14.93	1982.67
AB97-2		17/7/03		15.28	1982.32
AB97-2	0.032	17/7/03		15.63	1981.97
AB97-2		17/7/03		15.98	1981.62
AB97-2		17/7/03		16.32	1981.28
AB97-2		17/7/03		16.67	1980.93
AB97-2		17/7/03		17.02	1980.58
AB97-2		17/7/03		17.36	1980.24
AB97-2		17/7/03		17.71	1979.89
AB97-2		17/7/03		18.06	1979.54
AB97-2		17/7/03		18.41	1979.19
AB97-2		17/7/03		18.75	1978.85
AB97-2		17/7/03		19.10	1978.50
AB97-2		17/7/03		19.45	1978.15
AB97-2		17/7/03		19.79	1977.81
AB97-2		17/7/03		20.14	1977.46
AB97-2		17/7/03		20.49	1977.11
AB97-2		17/7/03		20.84	1976.77
AB97-2		17/7/03		21.18	1976.42
AB97-2		17/7/03		21.53	1976.07
AB97-2		23/7/03		21.88	1975.72
AB97-2		23/7/03		22.22	1975.38
AB97-2		23/7/03		22.57	1975.03
AB97-2		23/7/03		22.92	1974.68
AB97-2	0.060	23/7/03		23.26	1974.34
AB97-2		23/7/03		23.61	1973.99
AB97-2		23/7/03		23.96	1973.64
AB97-2		23/7/03		24.31	1973.29
AB97-2		28/7/03		24.65	1972.95
AB97-2		28/7/03		25.00	1972.60
AB97-2		28/7/03		25.35	1972.25
AB97-2		28/7/03		25.69	1971.91
AB97-2		28/7/03		26.04	1971.56
AB97-2		28/7/03		26.39	1971.21
AB97-2		28/7/03		27.08	1970.52
AB97-2		28/7/03		27.43	1970.17
AB97-2		28/7/03		28.47	1969.13
AB97-2		28/7/03		28.82	1968.78
AB97-2		28/7/03		29.17	1968.44
AB97-2		28/7/03		29.51	1968.09

AB97-2		28/7/03		29.86	1967.74
AB97-2		28/7/03		30.21	1967.39
AB97-2		28/7/03		30.55	1967.05
AB97-2		28/7/03		30.90	1966.70
AB97-2		28/7/03		31.25	1966.35
AB97-2		28/7/03		31.59	1966.01
AB97-2		28/7/03		31.94	1965.66